DISSOLVED OXYGEN AND pH MONITORING WITHIN CELL CULTURE MEDIA USING A HYDROGEL MICROARRAY SENSOR

A Dissertation

by

SEUNG JOON LEE

Submitted to the Office of Graduate Studies of
Texas A&M University
in partial fulfillment of the requirements for the degree of

DOCTOR OF PHILOSOPHY

December 2006

Major Subject: Biomedical Engineering

DISSOLVED OXYGEN AND pH MONITORING WITHIN CELL CULTURE MEDIA USING A HYDROGEL MICROARRAY SENSOR

A Dissertation

by

SEUNG JOON LEE

Submitted to the Office of Graduate Studies of
Texas A&M University
in partial fulfillment of the requirements for the degree of

DOCTOR OF PHILOSOPHY

Approved by:

Chair of Committee,	Gerard L. Coté
Committee Members,	Alvin T. Yeh
	Kenith Meissner
	Steven Wright
Head of Department,	Gerard L. Coté

December 2006

Major Subject: Biomedical Engineering

ABSTRACT

Dissolved Oxygen and pH Monitoring within Cell Culture Media

Using a Hydrogel Microarray Sensor.

(December 2006)

Seung Joon Lee, B.S., Yonsei University, Korea;

M.S., Texas A&M University

Chair of Advisory Committee: Dr. Gerard L. Coté

Prolonged exposure of humans and experimental animals to microgravity is known to be associated with a variety of physiological and cellular disturbances. With advancements in aerospace technology and prolonged space flights, both organism and cellular level understanding of the effects of microgravity on cells will become increasingly important in order to ensure the safety of prolonged space travel. To understand these effects at the cellular level, on-line sensor technology for the measurement and control of cell culture processes is required. To do this measurement, multiple sensors must be implemented to monitor various parameters of the cell culture medium. The model analytes used in this study were pH and dissolved oxygen which have physiological importance in a bioreactor environment. In most bioprocesses, pH and dissolved oxygen need to be monitored and controlled to maintain ionic strength and avoid hypoxia or hyperoxia. Current techniques used to monitor the value of these parameters within cell culture media are invasive and cannot be used to make on-line

measurements in a closed-loop system. In this research, a microfabricated hydrogel microarray sensor was developed to monitor each anlyte. Either a pH or an oxygen sensitive fluorescent agent was immobilized into a hydrogel structure via a soft lithography technique and the intensity image of the sensor varied from the target analyte concentration.

A compact detection system was developed to quantify concentration of each analyte based on the fluorescence image of the sensor. The system included a blue LED as an illumination source, coupling optics, interference filters and a compact moisture resistant CCD camera. Various tests were performed for the sensor (sensitivity, reversibility, and temporal/spatial uniformity) and the detection system (temporal/spatial stability for the light source and the detector). The detection system and the sensor were tested with a buffer solution and cell culture media off-line. The standard error of prediction for oxygen and pH detection was 0.7% and 0.1, respectively, and comparable to that of commercial probes, well within the range necessary for cell culture monitoring. Lastly, the system was coupled to a bioreactor and tested over 2 weeks. The sensitivity and stability of the system was affordable to monitor pH and dissolved oxygen and shows potential to be used for monitoring those analytes in cell culture media non-invasively.

DEDICATION

This dissertation is dedicated to my parents opening my eyes to the world and my wife the love of my life…

ACKNOWLEDGMENTS

The biggest thanks must go to my lovely wife, Youngmi, whose sacrifice and patience made this possible. I also want to thank my advisor, Dr. Gerard Coté, for his financial support, guidance, and patience throughout the years. Another special thanks goes to my other committee members, Dr. Kenith Meissner, Dr. Alvin Yeh, and Dr. Steven Wright, for their guidance, patience, and understanding. Several others helped in one way or another around the Optical Bio-sensing Laboratory: Bennett Ibey, Hope Beier, Becky Rounds. Another thanks goes out to the Chemical Engineering Department of Pennsylvania State University; Dr. Michael Pishko provided a wealth of information about soft lithography technique and chemistry. Finally, I would like to thank the National Aeronautics and Space Administration (NASA) who made the last several years financially feasible.

TABLE OF CONTENTS

CHAPTER Page

LIST OF FIGURES

FIGURE Page

FIGURE Page

LIST OF TABLES

CHAPTER I

INTRODUCTION

An Overview

Since astronaut crew time constraints are at a premium, microgravity biotechnology experiments on the NASA Space Shuttle and International Space Station (ISS) need to be minimized. Thus, compact and automated sensors are desired for assessing the health of cells during a bioreactor cell culture experiment. Several key metabolic parameters are routinely measured in order to check the health of cells, including pH and dissolved oxygen. Changes in these parameters can indicate culture growth, metabolism, as well as the problems with cells such as starvation, hypoxia, bacterial contamination.

Several single-analyte sensors have been developed for pH or dissolved oxygen monitoring [1-6]. Most sensors are either optical or electrochemical, or a combination of the two. While many single-analyte sensors perform adequately in bioprocess monitoring, the use of a multi-analyte sensor can simplify the measurement process by providing a single access point (decrease the chance of contamination), a single interface (easy data collection), and potentially reduce power consumption of the bioreactor system. Moreover, the use of any possible noninvasive sensor will decrease the chance of contamination compared to an invasive sensor.

This dissertation will describe in detail the development of a multi-analyte

---

This dissertation follows the style and format of *Journal of Biomedical Optics*.

monitoring system specifically designed for pH and dissolved oxygen in cell culture media. In terms of sensor development, pH and dissolved oxygen sensitive hydrogel microarrays were fabricated via soft lithography. The hydrogel was designed to allow mass transfer of the analyte from the surrounding media into the hydrogel where it would interact with an analyte sensitive fluorophore which is immobilized within the hydrogel structure. In terms of the detection system, a compact optical imaging system was developed to capture the fluorescence image from the sensor. The system includes an LED as an illumination light source, a CCD camera as a detector, and several optical filters to capture wavelength selective fluorescence images. The system was initially tested with buffer solution and cell culture media off-line. Finally, the monitoring system was coupled to a bioreactor and tested over 2 weeks.

Animal Cell Culture and Bioreactor

The first successful animal cell culture was reported by Ross G. Harrison in 1907 [7]. During several weeks, he studied the growth of nerve tissue from a frog embryo. Since then, animal cell culture has been widely used for investigation of cell physiology and biochemistry, production of artificial tissue, and production of biochemical products such as vaccines, enzymes, antibodies and hormones [8-10]. Use of cell culturing has been rapidly enhanced by the progress of genetic engineering [11].

Current efforts in biotechnology to produce transplantable artificial tissues will potentially benefit many patients suffering from tissue loss or organ failure [12]. Currently, more than 20,000 people receive transplanted organs, however, 6,000 patients

died waiting for an organ that did not come [13,14]. Because the supply of various organs is limited in the US, less than one half of the estimated 70,000 people in need of an organ will ever receive one. In addition, despite continuing advances in medicine and biotechnology, the demand for critical organs drastically outways the number of organ donors [13]. Hence, cell culture research has been motivated by the fact that organ donors are short in demand and mechanical devices cannot perform all of the functions of the organ. However, testing is underway on artificial organs such as pancreas, liver and kidney. A potential supply of replacement cells and tissues may come out of work currently being done with both embryonic and adult stem cells. These are cells that have the potential to differentiate into a variety of different cell types. It is hoped that learning how to control the development of these cells may offer new treatment approaches for a wide variety of medical conditions.

Cell based Pharmaceutical manufacturing is another field that benefits from research in cell culturing. While cultured cells can be used to produce many important products, two areas are generating the most interest. The first is the large-scale production of viruses for use in vaccine production. These include vaccines for polio, rabies, chicken pox, hepatitis B and measles [15-19]. Second, is the large-scale production of cells that have been genetically engineered to produce proteins that have medicinal or commercial value. These include monoclonal antibodies, insulin, hormones, etc [20-22].

Bioreactors are widely used for cell cultivation with controlled environmental conditions in cell culture procedures. The control of environmental conditions is

extremely important for mammalian cell culture. Since the animal cells are grown in cell culture media and covered by a phospholipid bilayer containing many kinds of enzymes and proteins, small changes in osmotic pressure, pH, hydrodynamic forces and nutrient concentrations may cause serious damage to the cells [23]. In addition, the control of the concentration of nutrients such as glucose, amino acids and growth factors, byproducts such as lactate and ammonia, and gases such as oxygen and carbon-dioxide in the cell culture media is essential for maintaining proper cell growth. Bioreactor systems can be used to potentially help solve these problems by controlling environmental conditions with the use of an on-line monitoring system. The ideal design for a bioreactor would allow for control of these parameters automatically in order to optimize cell growth.

The National Aeronautics and Space Administration (NASA) biotechnology program has used a Rotary Cell Culture System (RCCS) for cell cultivation [24]. The bioreactor produces three-dimensional cell culture growth in a ground based simulated microgravity environment that decreases the opportunity of cellular damage by suspending the cell aggregate within the central region of the bioreactor vessel. This microgravity environment allows the cells to use their energy expenditure on growth and reproduction rather than repair, resulting in a production of fully developed cells. However, current techniques used by NASA to monitor cell culture parameters are invasive and cannot be used in a closed-loop system because the sample has to be withdrawn from the bioreactor and analyzed with a commercial sensor. This increases the chances of contamination, is not appropriate for continuous monitoring, and needs manual intervention and consumes media. These are critical drawbacks, especially for

the space mission, and therefore a bioreactor equipped with an on-line and noninvasive monitoring system to control the cell culture environment is desirable.

Analyte Monitoring of Cell Culture Media

Monitoring pH

It has been shown that the changes in the pH of the extracellular cell culture environment can affect the performance of the culture [25,26]. Therefore, monitoring and regulating the pH of the media is one of the key steps in the success of the bioprocess. Physiological pH is optimally 7.0-7.7 within cell culture and differs for various cell strains. For instance, some normal fibroblast lines have optimal pH of 7.4-7.7 and transformed cells have a tendency to do better at 7.0-7.4 [27]. Cell culture media usually has some buffering capacity within the solution with the incorporation of sodiumbicarbonate. Despite the buffering capacity if the pH decreases or increases out of the optimal range it can have adverse effects such as influences on cell proliferation, metabolism [28], enzyme activity [29], product yield, and morphology [30,31]. It has also been shown that low pH can play a role in tumor initiation [32].

For most cell culture purposes, culture media contains phenol red, a pH indicator, which ranges in color depending on pH (i.e. orange (pH 7.0) to purple (pH 7.5.)). This allows for the subjective determination of pH by an individual engaging in small scale cell culture. In a bioreactor, however, pH is determined either off-line through sampling or real-time with the use of electrode [33]. The general form of such a sensor is a transducer element with a catalyst containing chemistry that provides an electrical signal

proportional to the pH. These sensors, however, need frequent recalibration, and are generally not compatible with bioreactor experiments because of difficult sterilization techniques, limited lifetimes, lack of stability, and binding of proteins to the sensor probe. Furthermore, the electrode can be subject to contamination because of the required port between the media and air. An alternative technique would be to used an optical sensor. Optical pH sensors are more suitable for bioreactor experiments because they use noninvasive techniques. They can be broadly classified as absorption and fluorescence based. The pH sensitive molecule, either absorptive or fluorescent, is loaded onto a solid matrix such as a membrane, sol gel, or using hydrogel technology. pH sensor techniques that use an indicator loaded into the matrix, are susceptible to leaching and photobleaching of the indicator due to flow conditions and light illumination, respectively. Currently, those are the only useful methods for monitoring pH of cell culture media not containing phenol red indicator. Many investigators have developed fluorescence based pH sensors. For a pH indicator, fluorescein, FITC, carboxyfluorescein, coumarin-4, fluorescein sulfonic acid, HTPS, SNARF, or SNAFL has been used in the near neutral pH range [34-41]. The pH sensing rage can be expanded by a use of multiple indicators sensitive to acidic/neutral/basic solution [42]. In this study 2′,7′-bis-(2-carboxyethyl)-5-(and-6)-carboxyfluorescein–dextran conjugate (BCECF-dextran) was used as a pH indicator. Standard fluorescein isothiocyanate labeled dextran (FITC-dextran) was studied, but proved to photobleach far too quickly to produce reliable signal overtime [43]. To remedy this, a modified fluorescein based compound (BCECF-dextran) was chosen which has greater photostability than FITC-

dextran [44].

Monitoring Dissolved Oxygen

The monitoring dissolved oxygen concentration throughout the course of any cell culture experiment provides valuable information about the metabolism and health of the cells. In a self-contained system like a microgravity bioreactor, human maintenance is kept to a minimum via a closed system for the delivery of fresh media and gasses and the removal of waste media. Optimization of this process requires the successful detection and evaluation of important nutrients and waste products. Extreme values for dissolved oxygen can hinder cellular functions and if left unchecked can result in cell death as a result of anoxia (deficient oxygen) or oxygen toxicity (excess oxygen).

The commonly used oxygen sensors to date are primarily electrochemical sensors based on Clark-type oxygen electrodes [45]. The Clark electrode suffers from a variety of limitations including long-term instability, drifts in calibration, flow dependence, and susceptibility to electrical interferences when used in bioreactors. Optical fiber sensors based on luminescence quenching provide a promising alternative to amperometric methods in solving the problems mentioned above.

Bergman described the first oxygen sensor based on fluorescence quenching in 1968 [46], which was introduced into the medical field in 1975 [47]. The introduction of immobilized indicators was an important landmark in the development of optical sensors for continuous monitoring in biological fluids. Due to its great potential for widespread application, optical sensing has received much attention and very intensive studies in this

field have been carried out [48-51]. Optical oxygen sensors are based on the property of molecular oxygen quenching of fluorescence. The fluorescent probe molecules like tris(2,2V-bipyridyl)ruthenium(II), tris(1,10-phenanthroline)ruthenium(II), and tris(4,7-diphenyl-1,10-phenanthroline)-ruthenium(II), which have high quantum yield of fluorescence and long fluorescence lifetime, are usually encapsulated in a gas-permeable material such as silicone rubber [52-55], silica gels [56], sol-gels [57-60], and polymers [61-64], and also incorporated into an optical probe (e.g., optical fiber) tip. Upon irradiation of the luminescent molecules by a blue excitation beam, a red fluorescence is emitted with a long-lived relaxation due to metal-ligand charge transfer (MLCT) from the MLCT-band, which constitutes the lowest excited state to the ground state [65]. In the presence of oxygen, the fluorescence is reversibly and quantitatively quenched. Reversible quenching of the fluorescent dyes by oxygen has been found to obey the Stern-Volmer equation:

$$\frac{I_0}{I} = 1 + k_D[Q] \qquad (1.1)$$

where I_0 and I are the intensities of the fluorescence in the absence and presence, respectively, Q is the concentration of the quencher (oxygen), and k_D is the Stern-Volmer constant.

Most of the optical oxygen sensors use optical fibers as the probe tip and blue light emitting diodes (LED) as the light sources [66]. Some investigators have used glass capillaries [67] and radioluminescent (RL) light sources [68] for optical oxygen sensors.

Optical fiber based sensors have a similar sensing scheme as electrochemical probes because they need a fiber as an “optical wire” that induce the same problems of potential for contamination as electrochemical probes. Hence, in this study, chip-type hydrogel microarray oxygen sensors were used rather than fiber-type sensors because the sensor can be used wirelessly after being embedded into a bioreactor system.

Poly(ethylene glycol) Hydrogels

In this study poly(ethylene glycol) (PEG) hydrogels were used to make microarray sensor structure. PEG is nondegradable, hydrophilic polymer that has been widely used as a biomaterial to obtain biocompatibility because of its remarkable nonadhesivity towards protein and cells [69]. Typically, PEG has been incorporated onto biomaterial surfaces by surface grafting, plasma polymerization, or simple absorption of PEG-containing block copolymers [70-75]. Different molecular weight of PEGs could be easily converted into acrylates such as PEG diacrylate (PEG-DA), and polymerization of acrylated PEG in the presence of light and photoinitiator yields a highly cross-linked hydrogel network [76,77]. PEG hydrogels have a high equilibrium water content, which provides rapid transport of small molecules through the gel network, and it was demonstrated that porosity of PEG hydrogels can be easily altered [78-80]. The aqueous environment of PEG hydrogels is suitable for the encapsulation of various biomolecules such as proteins, fluorophores, and even whole cells [81-83]. Furthermore, as mentioned, PEG hydrogels have been shown to be both biocompatible and nonfouling in complex environments [84,85]. Due to these characteristics, PEG hydrogels have been evaluated

for in vivo use including implanted sensors, drug delivery devices, and cell transplantation [86-89]. In addition, photopolymerized PEG hydrogels served to both stabilize and immobilize enzymes, providing a protective environment for enzymes that inhibits degradation and fouling [90,91]. The optically transparent nature of PEG hydrogels also makes them suitable for various schemes when they are used in optical biosensor applications.

Soft Lithography

Recently, Whitesides and collegues have developed a set of microfabrication techniques that is an alternative to photolithography and more suitable for biological applications [92,93]. This technique is called "soft lithography" because all methods require the use of soft elastomeric materials for pattern transfer and modification in those techniques [94,95]. The soft lithography technique includes two common methods for micropatterning - microcontact patterning and microfluidic patterning. For microcontact patterning, an ink is spread on a patterned poly(dimethyl siloxane) (PDMS) stamp. The stamp is then brought into contact with the substrate, which can range from coinage metals to oxide layers. The ink is transferred to the substrate where it forms a self-assembled monolayer that can act as a resist against etching. For microfluidic patterning, microchannels are formed by bringing a patterned PDMS mold into conformal contact with a substrate. When a drop of solution containing biomolecules is placed on the substrate adjacent to the channel opening, capillary forces pulled the fluid into the channels and only microliters of solution is required to fill the microchannels. In this

study, a modified microfluidic patterning was used to create sensor structure because of its simplicity and fidelity to create 3-D structures. A schematic illustration for soft lithography including a master fabrication is shown in Figure 1.1 [94].

CHAPTER II

HYDROGEL MICROARRAY SENSOR FABRICATION

Introduction

The soft lithographic method allows easy fabrication of hydrogel structures into very small sizes and patterns by the use of an appropriate mask. The fabrication of an array of hydrogel structures containing different components on the same substrate would require a sequence of injection, exposure and alignment, adding to the complexity of fabrication. To overcome these problems, a pin printer (as is used to create gene-chips) was used to fabricate micron scale hydrogel structures which can be used for multi-analyte sensing applications [96,97]. However, the pin printing technique requires a modified pin printer which increases the cost for fabrication, and inherently, it is not easy to control size and height during fabrication. Hence, a modified microfluidic patterning approach was proposed to fabricate a multi-analyte sensitive hydrogel microarray to overcome the difficulties of conventional photolithographic techniques.

The first step, in the modified approach, is fabrication of a master on a silicon wafer with several channels with desired width, separation distance, and height. The next step is fabrication of PDMS molds with negative channels. After sealing the PDMS and substrate, different analyte sensitive agents are injected into different channels to allow for spatial separation. Finally, each agent solution is cured by exposure to UV light to form a multi-analyte sensitive array. The response of each element of the array can be monitored through single images of the sensor array.

The sensor was characterized in terms of functionality and reversibility. The

sensitivity was tested by measurement of intensity changes of each sensing element under different analyte concentrations. The reversibility was tested through several cycles of analyte concentration. In addition, several sensors were fabricated from a single PDMS mold and tested under the same conditions to ensure consistent fabrication of the hydrogel microarray.

Experimental Section

Reagents

Liquid poly(ethylene glycol) diacrylate (PEG-DA) with an average molecular weight of 575, 3-(trichlorosilyl) propyl methacrylate (TPM), 6 N sulfuric acid, n-heptane, and dichlorotris (1,10-phenanthroline) ruthenium(II) hydrate were purchased from Sigma-Aldrich (St. Louis, MO). 2′,7′-bis-(2-carboxyethyl)-5-(and-6)-carboxyfluorescein –dextran conjugate (BCECF-dextran, 70,000 MW) was purchased from Molecular probes (D-1880, Carlsbad, California). 2-Hydroxy-2-methyl-1-phenyl-1-propanone (Darocur® 1173) was obtained from Ciba Specialy Chemicals (Tarrytown, NY). Deionized water with a resistance of 18 MΩ·cm was used for all aqueous experiments (Millipore, Billerica, MA). Poly(dimethyl siloxane) (PDMS) elastomer was purchased from Dow Corning Sylgard 184 (Midland, MI), which is composed of a prepolymer and curing agent. SU-8 50 negative photoresist and developer was purchased from Microlithography Chemical Corp (Newton, MA). Phosphate buffer saline (PBS, 0.1M pH 7.4) consisted of 1.1mM potassium phosphate monobasic, 3mM sodium phosphate dibasic heptahydrate, and 0.15M NaCl in 18 MΩ·cm deionized water. All other

chemicals used were commercially available and used without further purification.

Fabrication of a Master and PDMS Replica

A key component for soft lithography is the PDMS mold. In order to make a PDMS mold with microchannels, an SU-8 master was designed and fabricated. As shown in Figure 2.1, a chrome sodalime photomask was designed with Autocad® (Autodesk Inc., San Rafael, CA) and purchased from Advanced Reproductions (Andover, MA). Three microchannels were designed with different channel width and channel separation (50, 100, 200 μm). To fabricate the masters, SU-8 50 photoresist was used to produce a positive relief of microchannels on silicon wafers (University wafers, Boston, MA) through the following procedures.

1. The silicon wafer was dehydrated in an oven at 200 ^{o}C over 5 minutes.
2. SU-8 50 was spin-coated on a silicon wafer for 20 seconds at 2000 rpm for 50 μm thickness (or 1000 rpm for 100 μm thickness).
3. SU-8 50 was soft baked at 95 ^{o}C for 20 minutes (30 min. for 100 μm thickness).
4. The wafer was exposed to UV light through the photomask which had the designed microchannel.
5. SU-8 50 was post baked at 95 ^{o}C for 5 minutes (10 min. for 100 μm thickness).
6. The wafer was immersed into the SU-8 developer for 6 minutes (10 min. for 100 μm thickness)
7. The wafer was rinsed with isopropyl alcohol (IPA)

8. The master was dried with compressed air or N_2
9. The master was hard baked at 150 ^{o}C for 10 minutes.

Masters were stored at room temperature under a dust free condition. Prior to every use, masters were cleaned with 75 % alcohol, dried with compressed air or N_2 and inspected under a microscope to ensure a flawless surface.

Once a master was fabricated, microchannels in PDMS were formed by replica molding. Figure 2.2 shows a scheme for the rapid fabrication of microchannels in PDMS. Replica molding is simply the casting of PDMS precursor against a master and the generation of a negative replica of the master in PDMS. PDMS precursor was prepared by mixing a PDMS prepolymer with curing agent in a 10:1 ratio by weight as per the manufacturer's instruction. Because of its high viscosity, bubbles were generated during mixing and removed by applying vacuum in a vacuum chamber for 5 minutes. This mixture was poured (very slowly to avoid bubbling) onto the silicon master placed in a petridish and then cured in an oven at 60 ^{o}C for least 1 hour or 12 hours at a room temperature. The replica was peeled off from the master and the master was reused to obtain an identical PDMS replica. After several replicas were produced, several holes were punched through the PDMS replicas using a 20-guage needle to access the microchannels. The punching was performed from the bottom of the PDMS (channel surface) to avoid any burrs on the channel inlet/outlet. The PDMS replica was inspected under a microscope to ensure flawless microchannel generation. Finally, the PDMS replica was rinsed with deionized water, cleaned with 75% alcohol, dried with

compressed air/N_2, and then stored at room temperature until required further experiments.

Functionalization of the Substrate

The modification of glass slides with TPM was performed using a standard protocol for silane surface modification [98]. A detailed procedure is described below:

1. Cut glass slides to desired sizes.
2. Place glass slides into a "piranha" solution consisting of a 3:1 ratio of H_2SO_4 and H_2O_2 (*caution: this mixture reacts violently with organic materials and must be handled with extreme care*).
3. Wait 5 hours to clean glass surfaces.
4. Pick up one or two slides, rinse off acid with deionized water, check for water beading indicating a hydrophobic surface.
5. Leave slide in solution for a few more hours if water does not bead.
6. Rinse all remaining slides several times with deionized water to remove any acid solution.
7. Place glass slides into a 1M NaOH solution individually to coat both sides of each slide
8. Wait 5-12 hours for silanization.
9. Rinse slides several times with deionized water to remove any NaOH solution (water should spread out (not bead) because of hydrophilic surface).

10. Rinse slides several times with ethyl alcohol to remove any water.
11. Prepare a 1mM solution of TPM in a 4:1 ratio of heptane-carbon tetrachloride.
12. Drop each slide into the TPM solution individually.
13. Wait 5 minutes to allow TPM to form a single layer on the surface.
14. Rinse each slide individually with ethyl alcohol and then deionized water.
15. Water should bead very well because of a hydrophobic surface.
16. Dry each slide with compressed air or N_2.
17. Store each slide under a dust free condition.

Fabrication of PEG Hydrogel Microstructures

Hydrogel microstructures were prepared from PEG-DA (MW 575) and 2-Hydroxy-2-methyl-1-phenyl-1-propanone (Darocur® 1173), which was used as a photoinitiator. Chemical structures of these two chemicals are shown in Figure 2.3. After functionalization of the microscope glass slide with TPM, the PDMS replica with six microchannels was placed on the glass side and then dehydrated in an oven at 60 ^{o}C for 24 hours to seal the microchannels. Precursor solution consisting of PEG-DA (60% v/v), photoinitiator (2% v/v), and deionized water (38% v/v) was then injected into each microchannel with a 20-gauge syringe needle. For an array fabrication, a photomask, previously used for master and PDMS fabrication, was placed on a modified microscope stage. As depicted in Figure 2.4, a microscope was modified with an optical system to have collimated the UV light for uniform exposure throughout the photomask. In short,

the fiber tip of UV light source was clamped by a fiber holder, a collimating lens (f = 50 mm) was placed in front of the fiber, a flat glass mirror was placed under a microscope stage for beam reflection, and the microscope stage was fabricated to have larger illumination area covered with rubber to prevent the mask from slipping. A schematic diagram for fabrication of the microarray is shown in Figure 2.5. In detail, the PDMS replica on a glass slide was placed on the photomask and aligned under the microscope such that the microchannels of the PDMS were perpendicular to channels on the photomask. The hydrogel microarray was formed by exposing the precursor solution to UV light (EFOS Ultracure 100SS Plus, Ontario, Canada) for 2 seconds. Finally, the PDMS replica was removed quickly and the remaining unpolymerized hydrogel precursor solution was removed by rinsing with deionized water. The hydrogel microarray was stored in a buffer solution (PBS 0.1 M, pH 7.0) to avoid dehydration of the microarray. The hydrogel microarray sensor was characterized under a microscope (Leica DMLM, Leica Microsystems Inc, IL). A physical inspection was performed with bright field images. Reproducibility of the sensors was tested by fabrication of multiple sensing arrays from a single PDMS replica.

Characterization of Multi-analyte Sensitive Hydrogel Microarray Sensor

In order to fabricate a multi-analyte sensitive microarray, two different precursor solutions were prepared. For the pH sensitive elements, the precursor solution was made by mixing PEG-DA (60% v/v), photo-initiator (2% v/v), BCECF-dextran solution at 2 mg/mL concentration (10% v/v), and deionized water (28% v/v). For the oxygen

sensitive elements, the precursor solution was made by mixing PEG-DA (60% v/v), photo-initiator (2% v/v), ruthenium complex solution at 5 mg/mL concentration (2% v/v), and deionized water (36% v/v). The ruthenium complex solution was previously made by dissolving dichlorotris (1,10-phenanthroline) ruthenium(II) hydrate power into a 4:1(v:v) mixture of methanol and toluene to a 5 mg/mL concentration. Precursor solutions were injected into different microchannels to generate spatially separated sensing elements. Photopolymerization was then performed in same manner as described previously.

In order to test functionality of the microarray sensor, the sensor was immersed in a series of sample solutions, and fluorescence images were captured under a microscope by a CCD camera. A tungsten-halogen light source was used with a band pass filter (λ_{center} = 470 nm, λ_{FWHM} = 20 nm) for excitation and a 500 nm cut-off long-pass filter was used to capture the fluorescence image. Four different buffer solutions (PBS 0.1M) with either pH 6.0 or pH 8.0 and either 0% or 21% dissolved oxygen were prepared by adding HCl/NaOH and bubbling air/N2 continuously. Each sample was placed under the microscope and the sensor was immersed in the sample. There was at least a 10 minute delay between each test because it was expected that the response time of the sensor would be limited by natural diffusion of analyte within the hydrogel structure. A target element was selected and aligned at the center of the microscope view to insure consistent exposure to the sensor array. In addition, reproducibility of the sensor was tested by fabrication of multiple sensors from a single PDMS replica. The test was performed by immersing multiple sensors in a sample solution, aligning each

target element at the center of microscope view, and collecting image data.

Results and Discussion

Fabrication of a Master and PDMS Replica

In order to fabricate the PDMS replica, the SU-8 master was fabricated with desired channel width and height. SU-8 is an epoxy based negative photoresist. Upon exposure to UV light, cross-linking proceeded in two steps: formulation of a strong acid during the exposure, followed by acid-initiated, thermally driven, epoxy cross-linking during the post exposure bake [99]. Therefore, when SU-8 coated silicon wafers are exposed to UV light through the photomask, only exposed regions are cross-linked and become insoluble to developer solution. The height of structure can be controlled through the spin coating speed as well as the use of different viscosities of SU-8. Generally, to fabricate thicker/thinner structures, the use of SU-8 with higher/lower viscosity is required. The specific product name used for this study is SU-8 50 which has a viscosity of 12250 cSt and is able to generate 40 ~ 100 μm thicknesses with 3000 ~ 1000 rpm spin coating, respectively. Figure 2.6 shows an example of a master, used for this study, which has 100 μm channel width, 100 μm channel separation, and 50 μm channel height. The structure of SU-8 was chemically/physically stable and could be used many times without degradation in shape.

After the fabrication of masters, microchannels in PDMS were formed using replica molding by casting of PDMS precursor against a master. To form enclosed channels, PDMS was sealed to the glass slide by dehydration. Figure 2.7 shows an

example of PDMS placed on a glass slide. The seal between the PDMS and the glass slide was sufficiently strong so that the two substrates could not slide easily and could withstand injection pressure without leakage of flow. However, PDMS was easily peeled off from the glass slide with moderate force and without leaving any PDMS residue on the substrate. Therefore, we were able to use a single PDMS numerous times without functional degradation or deformation. In addition, we were able to observe microchannels inside the PDMS with an optical microscope and easily align the channels to the photomask since PDMS is optically transparent to visible light.

Functionalization of the Substrate

Without an adhesion promoting monolayer, even though microstructures could be developed, surface attachment was weak and array elements easily delaminated upon hydration due to swelling of the cross-linked hydrogel structure. To prevent delamination, a self assembled monolayer of TPM on the glass substrate was used to create a reactive surface onto which the hydrogel was covalently affixed during photopolymerization. The treatment of glass surface with chlorosilanes or alkoxysilanes is a commen and effective way to form self-assembled monolayers [100,101]. From testing several sensor fabrications, it was determined that sensors were firmly affixed to the glass substrates and did not detach from slides under fast sample flow, slight scratching, or swelling due to hydration, which ensures strong covalent bonding between the hydrogel structure and the glass substrate.

Fabrication of PEG Hydrogel Microstructures

The formation of hydrogel structures from PEG-DA was based on the UV initiated free-radical polymerization of acrylate end groups on the PEG-DA and substrate [80]. As shown in Figure 2.8, the photoinitiator used in this study, was dissociated upon exposure to UV light, creating highly reactive methyl and benzaldehyde radicals, which then attack the carbon double bond (C = C) of acrylate on the macromer, thus initiating free radical polymerization. Since two reactive centers per macromer are created, propagation results in the formation of a highly cross-linked PEG structure. This structure produces three-dimensional insoluble structures, capable of entrapping sensing agents. The methacrylate surface (TPM modification) of substrates will also take part in the polymerization because it contains an unsaturated carbon double bond. Methacrylate groups on the surface of substrates react with radicals near the surface to effectively anchor the hydrogels to the surface of the glass substrates. Thus, delamination or detachment of PEG hydrogel structure from the substrate was significantly reduced.

Hydrogel microarrays were fabricated with a soft lithographic technique. Figure 2.9 shows an array of hydrogel structures. Clearly defined three-dimensional structures with no residual polymer remaining on the substrate were observed. The Figure also shows a very smooth surface without any visible defects in the polymer network. In addition, under bright field images, no difference was observed visually between elements containing agent and elements with PEG only.

Characterization of Multi-analyte Sensitive Hydrogel Microarray Sensor

It is well known that BCECF-dextran and dichlorotris (1,10-phenanthroline) ruthenium(II) hydrate are reversibly sensitive to pH and dissolved oxygen in a solution, respectively [102,103]. The chemical structures and absorption/emission spectra are shown in Figure 2.10. Both agents absorb blue light and emit different intensities of green or red fluorescence light depending on pH or dissolved oxygen changes, respectively. Hence, we were able to use a single light source for excitation and use single optical filter (500 nm cut-off longpass filter) for fluorescence detection, resulting in an uncomplicated detection system.

To be used as an analyte sensitive sensor, the hydrogel structure must stably encapsulate each agent within the structure without leakage of agent or obstruction to the target analyte. After the fabrication of the hydrogel microarray sensor with two different agents, the sensor was placed in several sample solutions with different analyte concentrations. As shown in Figure 2.11, the BCECF immobilized element shows different intensity at pH 6.0 and pH 8.0, regardless of dissolved oxygen level. The ruthenium complex immobilized element shows different intensity at 0% and 21% dissolved oxygen level, regardless of pH. This test was repeated several times to examine the reversibility of the sensor and similar images were obtained to reveal that the reversibility of each agent was not affected by immobilization. Any significant leaching or bleaching of the agent was not observed throughout the experiment.

One important problem for multi-analyte sensitive sensors will be the potential cross-effect between sensors. If there are any effects due to the concentration changes of

one analyte in sensor elements that are designed to be sensitive for other analytes, there could be large errors when the sensor is used for quantification of analytes. However, even though no visible cross-effect was observed, the cross-effect can not be determined with this study because it requires a reliable detection system. This will be discussed in other chapters. From these results, it was confirmed that analyte sensitive agents were successfully immobilized into the hydrogel structure without loosing their functionality.

Conclusion

This chapter described the fabrication technique of a PEG hydrogel microarray using modified soft lithography that has potential applications in multi-analyte biosensing. Construction of a master slide on a silicon wafer was performed by using a commercially available SU-8 protocol and this pattern was transferred into a PDMS mold. Sandwiching this mold onto a silica wafer created microchannels that were filled with a PEG polymer precursor solution. Using a customized UV curing system portions of the channels were selectively polymerized using a mask placed orthogonal to the flow. This process provided a very accurate method for generating sensing arrays on the micron level. Using this method it is not only possible to construct large uniform arrays, but arrays that contain multiple sensing elements. The ability to construct multiple sensing elements on a single small array is paramount to the realization of the project goal of creating an indwelling multi-analyte sensor for automated cell culturing.

CHAPTER III

FLUORESCENCE IMAGING SYSTEM FOR THE HYDROGEL MICROARRAY SENSOR

Introduction

Most fluorescence sensors convert concentration of the target to fluorescent intensity by applying it to a pre-calculated calibration model. In order to predict analyte concentration with a sensor, a stable and reliable sensing system is required because a systemic error or variation can cause a tremendous prediction error.

The detection system used for this study can be divided into two parts: illumination and image detection. An LED was used for illumination and a CCD camera was used for image detection. Both electrical products are temperature sensitive. Heating or cooling changes the electrical conductivity of certain parts inside the equipment causing systemic error or noise. In order to characterize the custom imaging system, sensing arrays were created as per the procedure describe in Chapter II. Both temporal and spatial uniformity of the illumination light source and detector were tested. In addition, spatial uniformity of the sensor array was tested using the optical system. The following chapter describes the methods and results obtained while engineering and constructing the custom optical imaging system.

Experimental Section

Reagents and Equipment

All the chemicals used for fabrication of master, PDMS replica, and hydrogel sensors were described in chapter II. They were commercially available, and used without further purification. A monochrome CCD camera with 10-bit dynamic rage and 1392×1040 pixels was purchased from Hitachi (KP-F100B, Hitachi Kokusai Electric America, Woodbury, NY). A blue LED with 7^{o} half intensity beam angle (λ_{peak} = 470 nm, λ_{FWHM} = 40nm) was obtained from Opto Diode Corp. (Newbury Park, CA) and served as an excitation light source. A digital power supply (HP, Palo Alto, CA) was used for precise control of the LED. Three optical filters were used, one for illumination (λ_{center} = 470 nm, λ_{FWHM} = 20 nm), one for blocking illumination light (500 nm longpass), and one for fluorescence emission (λ_{center} = 560 nm, λ_{FWHM} = 100 nm). All filters were purchased from Chroma Technology Corp (Rockingham,VT). A quartz flow cell (face detachable) with 2 mm pathlength (Starna Cells, Atascadero, CA) was used as a sample chamber and sensor holder. Other components included an optical power meter (Coherent Inc., Santa Clara, CA) PVC tubing (VWR, West Chester, PA), peristaltic pump (VWR), one-way check valve and luer fittings (Value Plastics Inc., CO).

Hydrogel Microarray Fabrication

The PEG-based pH and oxygen sensor was constructed using a modified procedure to bind PEG hydrogels to glass substrate. The detailed fabrication method was described previously in chapter II. In short, the hydrogel arrays were patterned photo

lithographically with PEG-DA on to glass substrates. To prepare the substrates for the hydrogel microstructures, an oxidized surface was created by using a sulfuric acid wash for 4 hours, followed by a sodium hydroxide 1 M wash for at least 4 hours. The oxidized glass was treated with 3-(trichlorosilyl)propyl methacrylate (TPM) in a hexane and carbon tetrachloride mixture (3:1). In this study, single analyte sensitive sensors were fabricated for uniformity tests. Two different precursor solutions were prepared for each analyte. For the pH sensitive sensor, the precursor solution was made by mixing PEG-DA (60% v/v), photo-initiator (2% v/v), BCECF-dextran solution at 1 mg/mL concentration (10% v/v), and water (28% v/v). For the oxygen sensitive sensor, the precursor solution was made by mixing PEG-DA (60% v/v), photo-initiator (2% v/v), ruthenium complex solution at 5 mg/mL concentration (2% v/v), and water (36% v/v). The concentration of each fluorophore was previously determined to have similar fluorescence dynamic range under experimental conditions. The volume ratio of PEG-DA and photoinitiator was kept constant to ensure identical hydrogel structure for each sensor. The PDMS made using the above procedure was affixed to the treated glass slide and allowed to dehydrate for 24 hours. Precursor solution was injected into three microchannels and cured by UV light (EFOS Ultracure 100SS Plus) that was projected through the chrome photomask for 2 seconds (300 mW/cm^3, λ_{peak} = 365 nm) to form single analyte sensitive hydrogel arrays. After curing, the PDMS replica was removed from the glass slide and the slide was washed to remove uncured solution. The final sensor contained identical 3×3 arrays. The excess glass surrounding the array was removed by cleaving to reduce the size of the final sensor.

Fluorescence Imaging System

An optical detection system was designed to capture the fluorescence image of the sensor array. As depicted in Figure 3.1, a blue LED was used as the illumination source for the sensor array. The LED was powered by a digital power supply for an accurate voltage control. A custom designed heat sink was made for the LED as per the manufacturer's recommendation. Since the LED spectrum is too broad for fluorescence applications, a bandpass filter (λ_{center} = 470 nm, λ_{FWHM} = 20 nm) was placed in front of the LED to shorten the spectral range. A lens with a 50 mm focal length was used to focus the light onto the sensor. As shown in Figure 3.2 (side view of the flow cell), a quartz flow cell (face detachable) with a 2 mm pathlength was used as a sample chamber and sensor holder. A silicon bumper was made by cutting a short (~3 mm) silicon tube in half to hold the sensor array in the flow cell. The bumper was narrow enough so as not to block the sample flow. The flow cell was then mounted on an xyz-positioner for easy and fast alignment and focusing. A rotation stage was mounted vertically on the positioner to compensate for any tilting of the sensor array. The flow cell was connected to a peristaltic pump for sample perfusion. The flow direction was set from bottom to top of the flow cell for easy bubble removal. A one-way check valve was placed between the pump and the flow cell to avoid a backflow. A microscope objective lens (10X) was used to focus the sensor image onto a CCD camera. A 500 nm cut-off longpass filter and a bandpass filter (λ_{center} = 560 nm, λ_{FWHM} = 100 nm) were used to remove the excitation light. The CCD camera was connected to a PC, controlled by EPIX® program (EPIX Inc., Buffalo Grove, IL) and all captured images were imported to MATLAB® (Natick, MA)

for further analysis.

Characterization of the Imaging System

In order to characterize the imaging system, several tests were performed. For stable illumination of the sensor the LED was tested by measuring the intensity using an optical power meter. The power supply was set to voltage control mode for a constant voltage input. The test was performed twice at 3 V and 3.5 V input to the LED. In addition, the temperature of LED was monitored using a digital thermometer. There was a 2 hour cooling time for the LED cooling test. The beam uniformity was tested by capturing blank images without the sensor. In order to increase the beam uniformity, a diffusion film was placed in front of the flow cell. In a previous study it was observed that the temperature of the CCD camera was increased after electricity was supplied. Temperature stability of the camera was tested by capturing images every three minutes for an hour at various temperatures.

Spatial and Temporal Uniformity of the Sensor

For the spatial uniformity test, two different sensors were fabricated with either pH or oxygen sensitive agent. Each sensor set includes a 3×3 array and each element has 100 μm width and 100 μm channel separation. After placing each sensor in the flow cell, a buffer solution (PBS 0.1M pH 7.0) was prepared and continuously flowed through the flow cell by a peristaltic pump. Compressed air was bubbled into the solution to keep the dissolved oxygen level at 21%. The oxygen level was confirmed by a commercial

oxygen sensor and pH was confirmed by a commercial pH sensor. As shown in Figure 3.3, the pH sensor was aligned to have the center element positioned at the center of the camera image. The sensor image was captured and the sensor position was moved either up, down, right or left by 100 μm. This movement was performed easily by the scaled xyz-positioner. Another image was captured after movement. This step was repeated until the last element was positioned at each corner. A total number of 25 (5×5) images were collected. Each image was cropped to contain 9 elements (3×3) resulting in an image size of 50 by 50 pixels (total 2500 pixels). The average intensity value and standard deviation within each element was calculated. The same test was performed after the pH sensor was replaced by an oxygen sensor.

Results and Discussion

Characterization of the Imaging System

Unlike typical LEDs, the high powered LED (1200 mW energy dissipation at 300 mA, 25 ^{o}C) used for this study generates significant heat while being powered. After supplying electricity to the LED, as shown in Figure 3.4, the temperature of the LED, current, and intensity were increased. However, all parameters were stable after 20 min. and 12 min. in the case of 3 V and 3.5 V inputs, respectively. Faster stabilization was observed at higher voltage input because more energy was dissipated from the LED. The stabilized values of temperature, current, and intensity were 26.1 and 33.5 ^{o}C, 75 and 411 mA, and 5.18 and 19.8 μW at 3 and 3.5 V input, respectively. Afterwards, based on this result, there was at least 30 minutes of stabilization time for the LED before each

experiment. Once stabilized, the intensity of LED remained constant without any fluctuation or drift over two weeks.

Since the LED beam profile is typically not uniform, the beam focusing lens was adjusted (defocused) to have a maximized uniform beam on the sensor rather than focusing the beam on the sensor. In order to increase the beam uniformity, a diffusion film was placed in front of the flow cell. The filter, used for the LED, was removed during the test because the imaging system was designed to capture a fluorescence image rather than the LED. Figure 3.5 shows the results from the beam uniformity test. Without a diffusion film, the beam profile was heavily gradient to the center. There was about 6.8 % intensity difference between the center area and the side area. After using the diffusion film, overall intensity was dropped due to more absorption/scattering by the diffusion plate, but the beam uniformity was enhanced by 3.5 % intensity difference. It was quite difficult to get a uniform beam with the current optical setup. However, this problem can be solved by relative measurement or background subtraction as long as temporal stability is confirmed.

The CCD camera is also temperature sensitive. As shown in Figure 3.6, as temperature increases, the standard deviation of multiple pixel values (cropped from center of CCD with 500×500 pixels) was increased. After around 30 minutes, the signal and the temperature of the camera were stabilized. A CCD chip works by converting incoming photons of light into electrons, which are stored in the pixels and later converted to a digital signal. However, it turns out that electrons are not only produced by photons of visible light that strike the CCD chip. This phenomenon is called “dark

noise" caused from electrons that are generated in the absence of light, as a result of heat produced by the CCD chip itself. These electrons create hot pixels which increase in intensity over the exposure duration, and which can be minimized by consistent cooling of the CCD chip. Even though many cooled CCD cameras are commercially available they can not be used for this application because the ultimate goal of this system is for it to be operated inside of an incubator at human body temperature with high humidity intended for optimal cell growth. A cooled CCD camera at high temperature or high humidity can cause significant water condensation which can cause malfunction or serious damage to the camera. However, average intensity was consistent over the experimental conditions which makes the CCD camera an acceptable option for this application.

Spatial and Temporal Uniformity of the Sensor

In order to ensure spatial uniformity of the sensor array, pH or oxygen sensitive microarrays with nine (3×3) identical elements were fabricated and each element was placed at a different position. It is well known that fluorescence intensity is proportional to the excitation light intensity. Therefore, it was expected that one target element would show a different fluorescence intensity at a different location, even at the same analyte concentration, because the beam profile was not uniform. Table 3.1 shows the intensity variation of pH sensitive elements at different locations. Even though there was variation at different locations, the intensities of nine elements at the same location was identical, which supports the fabrication consistency. This test was performed with a pH sensor as

well as oxygen sensor and similar results were obtained. As a result, the soft lithographic technique used to fabricate the multi-analyte sensitive hydrogel microarray yielded spatial/temporal consistency and shows the potential to be used for quantification of analyte concentration from fluorescence intensity.

Conclusion

In this chapter the optical system that was constructed to image the entire sensing array was described and data was provided that confirmed its functionality in terms of clarity of image and uniformity of illumination. The illumination of the sensing array was especially problematic optically due to the conical nature of the LED output. The system was sensitive to temperature but it was consistent once stabilized. A typical diffusion film enhanced beam uniformity and the data provided showed some uneven illumination across the imaging plane, however, it did not directly impact the overall results from the sensor. One possible way to eliminate this problem in the future is to use a uniform light source such as an LED backlight panel. However, it was not appropriate to use for this application because of spectral range mismatch and low intensity. Overall, the custom optical system performed very well and is capable of adequately collecting the data necessary for quantification of analyte concentration across multiple sensing elements.

CHAPTER IV

DISSOLVED OXYGEN AND pH SENSING WITH A HYDROGEL MICROARRAY SENSOR

Introduction

Previous research groups have shown that sensing using single element arrays and large single slab sensors are capable of measuring dissolved oxygen and pH using buffered solution with good accuracy [104]. The long term stability of these sensors has also been shown to be well within the limits of a standard cell culturing experiment. In this chapter a novel sensing array which contains two independent sensing elements is described and tested in both aqueous buffer and commercially available cell culture media using the custom optical imaging system described in chapter III. A calibration model for each analyte was obtained by measuring fluorescence intensity in a solution doped with a random concentration of each analyte. The validation was performed in the same manner as the calibration step and the performance was characterized using a standard error of calibration (SEC) and a standard error of prediction (SEP). In addition, the response time of the sensor was tested under rapid concentration changes for each analyte. A relatively slow response of the sensor was expected because the local concentration change within the sensing element was based on natural diffusion which is typically slow.

Experimental Section

Reagents

Minimum essential medium (MEM) without phenol red were purchased from Sigma-Aldrich (St. Louis, MO). Penicillin-streptomycin and fetal bovine serum was purchase from Gibco (Carlsbad, CA). All the chemicals used for fabrication of master, PDMS replica, and hydrogel sensors were described in chapter II. They were commercially available, and used without further purification.

Hydrogel Microarray Sensor Fabrication

Autocad® was used to devise a pattern of 6 parallel microchannels 100 μm wide and 100 μm apart. This pattern was then patterned to a chrome-quartz photomask by Advanced Reproductions. SU-8 50 was spin-coated (2000 rpm) onto a silicon wafer and the wafer was cured through the photomask using long-wavelength UV to create a pattern on the silicon wafer with 50 μm height (based on manufacturer's instruction table). A PDMS mold containing microchannels (inverse of the pattern on the silicon wafer) was created by curing a 10:1 mixture of PDMS prepolymer and curing agent against the SU-8 50 patterned silicon. This mold was cured for 24 hours at 60 ^{o}C, removed, and extensively washed with water and 75% alcohol. Holes were punched on each side of the microchannels using a 20-gauge needle to create inlet ports.

The PEG-based pH and oxygen sensor was constructed using a modified procedure to bind PEG hydrogels to glass substrate. In short, the hydrogel arrays were patterned photolithographically with PEG-DA on glass substrates. To prepare the

substrates for the hydrogel microstructures, an oxidized surface was created by using a sulfuric acid wash for at least 4 hours, followed by a sodium hydroxide 1 M wash for at least 4 hours. The oxidized glass was treated with 3-(trichlorosilyl)propyl methacrylate (TPM) in a hexane and carbon tetrachloride mixture (3:1) to form a self assembled monolayer (SAM) with pendant methacrylate groups. Two different precursor solutions were prepared for each analyte. For the pH sensitive elements, the precursor solution was made by mixing PEG-DA (60% v/v), photo-initiator (2% v/v), BCECF-dextran solution at 1 mg/mL concentration (10% v/v), and water (28% v/v). For the oxygen sensitive elements, the precursor solution was made by mixing PEG-DA (60% v/v), photo-initiator (2% v/v), ruthenium complex solution at 5 mg/mL concentration (2% v/v), and water (36% v/v). The concentration of each fluorophore was previously determined to have similar fluorescence dynamic range under experimental conditions. The volume ratio of PEG-DA and photoinitiator was kept constant to ensure identical hydrogel structure for each sensor element. Both precursor solutions were mixed with a vortex mixer. The PDMS made using the above procedure was affixed to the treated glass slide and allowed to dehydrate for 24 hours. Precursor solution was injected into each microchannel and cured by UV light (EFOS Ultracure 100SS Plus) that was projected through the chrome photomask for 2 seconds (300 mW/cm^3, λ_{peak} = 365 nm) to form hydrogel arrays. After curing, the PDMS replica was removed from the glass slide and the slide was washed to remove uncured solution. The final sensor contained 2 arrays with 3 elements in each, allowing for the measurement of two independent chemicals in triplicate. The excess glass surrounding the array was removed by cleaving to reduce the

size of the final sensor.

Optical Imaging System

An optical detection system, describe in chapter III, was used to capture the fluorescence image of the sensor array. In short, a blue LED (λ_{peak} = 470 nm, λ_{FWHM} = 40nm) served as the illumination source for the sensor array. An optical bandpass filter was used as an excitation filter and a lens (f =50mm) served to focus the light on the sensor. A quarts flow cell with 2 mm pathlength was used as a sample chamber and sensor holder. The sensor was placed inside the flow cell and sample solutions were pumped over the sensor by a peristaltic pump. A microscope objective lens (10X) was used to focus the fluorescence image onto a monochrome CCD camera. A 500 nm cut-off longpass filter and a bandpass filter (λ_{center} = 560 nm, λ_{FWHM} = 100 nm) were used to remove excitation light. The CCD camera was controlled by a PC and all captured images were stored for data analysis. The voltage supply to the LED was set to 3.0V - 90mA to minimize photobleaching. The exposure time for all images was 2 seconds.

Characterization of the Hydrogel Microarray Sensor with Buffer Solution

As depicted in Figure 4.1, phosphate buffered saline solution (PBS, 0.1M) was placed into a beaker and a pH meter (Thermo, Waltham, MA) and a standard Clark electrode oxygen sensor (MI-730, Microelectrodes, Bedford, NH) were used to externally monitor pH and O_2. The commercial oxygen sensor was calibrated at the start of the experiment using two water standards; nitrogen gas (0% O_2) and air (21% O_2).

The commercial pH meter was calibrated with standard buffer solutions. To build the pH calibration model, pH was changed (pH 5.8 ~ 8.2) by adding acid/base in the solution while dissolved oxygen level was kept at 21% with continuous bubbling of air. The fluorescence image was captured and readings from the pH/oxygen electrode sensors were recorded. This step was repeated at 0% dissolved oxygen level. To build the oxygen calibration model, the oxygen level was changed (0~21%) by bubbling air/N_2 in the solution while the pH was kept at 6.0. The fluorescence image was captured and readings from the pH/oxygen electrode sensor were recorded. This step was repeated at pH 7.0 and pH 8.0, respectively. For validation, a table was made to have 20 spiked pH (6.0~8.0) and dissolved oxygen (3~21%) values with zero correlation. The pH and dissolved oxygen level of the solution was adjusted to follow the spiked sample table. Data was collected similarly for each pH and oxygen level.

Characterization of the Hydrogel Microarray Sensor with Cell Culture Media

In order to test the feasibility of the sensor to be used for real cell culture media during a bioprocess, another test was performed with cell culture media (typically used for mammalian cell culture). With the same experimental setup describe in the previous section, the buffer solution was replaced by minimum essential media (MEM) without phenol red, supplemented with 2 mM L-glutamine, 1.5 g/L sodium bicarbonate, 0.1 mM non-essential amino acids, 1.0 mM sodium pyruvate, antibiotics, and fetal bovine serum (10% v/v). A phenol red free media was chosen to avoid absorption variation due to color change of phenol red. Calibration and prediction data for MEM were collected in

the same manner as described in the previous section.

Sensor Response Time and Stability

Sensor response time was measured by continuous data collection during a rapid concentration change of each analyte. Sensor stability was tested by using a single sensor during the study. Between each experiment, the sensor was stored in a buffer solution under light tight conditions. All experiments were performed at constant room temperature. The sensor was sterilized with 75% alcohol prior to each experiment.

Results and Discussion

Characterization of the Hydrogel Microarray Sensor with Buffer Solution

To evaluate the sensor's sensitivity to each analyte of interest, the sensor was tested in buffer solutions with various pH/O_2 levels. For the pH sensor calibration, pH was gradually increased and decreased at a constant dissolved oxygen level and repeated for different constant dissolved oxygen levels. For the oxygen sensor calibration, dissolved oxygen was increased and decreased at a constant pH and was repeated at different constant pH values. Figure 4.2 shows the sensor response to pH and Figure 4.3 shows the sensor response to dissolved oxygen from the calibration data. Both sensors show sensitivity, repeatability and reversibility. Moreover, any strong evidence of optical/chemical cross-talk between sensors was not found. One major concern in fluorescence-based sensing is the photobleaching effect which is a permanent or semi-permanent destruction of the luminescent properties of the fluorescent probe. The

fluorescent emission of BCECF-dextran and ruthenium complex were stable under LED exposure during the experiment. Within the tested pH range (pH 5.8~8.2), no additional leaching (due to different degrees of swelling at different pH) was observed. Figure 4.4 and 4.5 show the calibration models for pH and oxygen, respectively. The pH sensor shows a sigmoidal response to pH which is nearly identical to free BCECF in solution [105]. A 3rd order polynomial fitting was applied to build the pH calibration curve. Within the tested pH range, 3rd order polynomial fitting successfully traced the pH sensor response (R=0.9989). Linear regression was applied to build the oxygen calibration model which agrees with the Stern-Volmer quenching model at low concentration (R=0.9969). For the prediction data, the intensity was applied to the calibration model and pH/O_2 was predicted and compared to the commercial electrode sensor reading. Figure 4.6 and 4.7 show the sensor response from the spiked sample data to pH and O_2, respectively. Both sensors show good sensitivity within the range of interest and show good agreement between the sensor and the commercial probe. Moreover, prediction plots of pH/O_2 sensors (Figures 4.8 and 4.9) show that both sensors are precise and unbiased. The standard error of calibration (SEC) and the standard error of prediction (SEP) were calculated as follows:

$$SEC = \left\{ \sum_{i=1}^{Nc} (c_i - \hat{c}_i)/(N_c - 1) \right\}^{1/2} \quad (4.1)$$

$$SEP = \left\{ \sum_{i=1}^{Ny} (y_i - \hat{y}_i)/N_y \right\}^{1/2} \quad (4.2)$$

Where c_i is the actual analyte concentration of the i^{th} sample in the calibration data set, $\hat{c}_i$ is the predicted analyte concentration, N_c is the total number of calibration data sets, y_i is the actual analyte concentration of the i^{th} sample in the prediction data set, $\hat{y}_i$ is the predicted analyte concentration, and N_y is the total number of prediction data sets. Table 4.1 shows the prediction results of pH and oxygen based on the fluorescence image from the spiked sample. Standard error of prediction (SEP) was 0.07 units for pH and 0.64 % for dissolved oxygen. Error sources include the response time of the sensor and/or delays in the flow-through system between the water bath and sensor array and differences between local pH/oxygen in the sensor and in the sample chamber because spiked sample testing requires rapid changes of pH or dissolved oxygen.

Characterization of the Hydrogel Microarray Sensor with Cell Culture Media

The sensor was tested in cell culture media to verify that the sensor can be used for bioprocess monitoring. Typically, cell culture media includes phenol red to monitor pH with color change. Since the excitation light passes through the media before the sensor array, a phenol red free media was used to avoid absorption variation from the

cell culture media. Calibration/prediction was performed in the same manner as previously described for the buffer solutions. The calibration data, as shown in Figures 4.10 and 4.11, shows similar results to the experiment with buffer solution. The R^2 values for the calibration model were 0.9976 for pH and 0.9931 for O_2, respectively.

As shown in Figures 4.12 and 4.13, the sensor responded to the spiked pH and dissolved oxygen without any noticeable bias or drift. As shown in Table 4.1, the standard error of prediction was 0.07 units for pH and 0.65 % for oxygen, which is nearly identical to the results with buffer. These results clearly show that the sensor was able to monitor pH and dissolved oxygen in a more complex media such as cell culture media. The sensitivity of the microarray sensor is comparable to the commercial electrode sensors (0.01 unit for pH and 0.1% for oxygen), but with the added advantages of being small and implantable, for noninvasive monitoring, rather than indwelling and tethered to the electronics.

Sensor Response Time and Stability

The sensor response time was tested by inducing a rapid change in the concentration of each analyte. As shown in Figure 4.14, 90% of the sensor's response was achieved in 48 seconds for a change in pH from 6.0 to 8.0 and 24 seconds for a change in dissolved oxygen from 21% to 0% which is slower than typical response time of commercial sensors (1~5 sec. for pH sensors and 5~10 sec. for oxygen sensors). The migration of a proton or oxygen molecule into the hydrogel structure is dominated by natural diffusion and presumed to be the reason for the slightly sluggish response time.

Therefore, this response time can be reduced by decreasing the size of each array to maximize the surface area to volume ratio. Alternatively, increasing the mesh size of the structure by using a decreased volume ratio of PEG-DA in the precursor solution would also speed up this diffusion, but may induce further leeching. The current response time shows the potential of the sensor to be used in bioprocess monitoring since it does not require the measurement of rapid analyte concentration changes.

After each experiment, the sensor was stored in buffer (PBS 0.01M, pH 7.0) without exposure to ambient light. The sensors used for the above experiments did not exhibit any noticeable photobleaching, dye leaching, or physical degradation over two weeks. The sensors were also sterilized with 75% ethanol and no loss in function was observed after multiple sterilizations. This data confirms that the sensor's lifetime is useful for a typical cell culture experiment and that the sensors can be sterilized, proving their potential for non-invasive monitoring.

Conclusion

This chapter described the response of the sensing array to variation in dissolved oxygen and pH in both aqueous buffer and cell culture media (the goal media). It is very important that the sensing array is able to quantify pH and dissolved oxygen in a simple media through a series of spiked solutions. The sensing element construct in this study responded well to random changes in pH and dissolved oxygen showing that the overall approach is very feasible in real world applications. The data was combined into a calibration and prediction model and the ability of the calibrated sensing system to

remain accurate over time was proven. For both buffer solution and cell culture media, the SEP and SEC for pH and oxygen sensor was around 0.7 and 0.6 %, respectively. The results for this sensor array in the more complex cell media solution where protein and other confounders are present were nearly ideal. Finally, in a separate test the overall response time of the sensing elements was seen to be under 1 minute, making it more than adequate for the relatively slow changing nature of cell culturing. The delay present in the sensors is attributed to the hindered diffusion of oxygen and protons through the PEG hydrogel.

CHAPTER V

ON-LINE MONITORING OF CELL CULTURE MEDIA WITH A HYDROGEL MICROARRAY SENSOR

Introduction

Previous chapters have described the fabrication and *in vitro* testing of a fluorescent sensing system utilizing an array of polymer hydrogels. This array was shown to sense two analytes (pH and dissolved oxygen) simultaneously with high accuracy. In this chapter, this system was tested in an *in vivo* environment using a cell culture bioreactor system. This system mimics that which would be implemented in fully automated space cell culture experiment. In an *in vivo* environment, the concentration of the analytes within the cell media change randomly due to the growth and metabolic needs of the cell culture. Unlike, the *in vitro* experiments, the random changes in the media concentrations can potentially confound the multi-analyte sensor. The experiments described in this chapter were performed to test the fluorescent systems feasibility and viability in a moderately controlled environment where small changes in analyte concentrations and environmental confounders can influence experimental results.

Experimental Section

Reagents

Cytodex® microcarrier beads, and Dulbecco's modified Eagle's medium (DMEM) without phenol red were purchased from Sigma-Aldrich (St. Louis, MO).

Trypsin-EDTA, penicillin-streptomycin, and bovine calf serum was purchase from Gibco (Carlsbad, CA). All the chemicals used for fabrication of master, PDMS replica, and hydrogel sensors were described in chapter II. They were commercially available, and used without further purification.

Fabrication of Hydrogel Microarray Sensor

pH and dissolved oxygen sensitive hydrogel microarrays were fabricated as described in chapter IV. In short, an SU-8 50 master was fabricated to have a pattern of 6 parallel microchannels with 100 μm width, 100 μm channel separation, and 50 μm height. A PDMS mold containing microchannels was created by curing agent against the SU-8 50 patterned master. TPM modified glass slides were prepared as substrates for the hydrogel microstructures. Two different precursor solutions were prepared for each analyte. For the pH sensitive elements, the precursor solution was made by mixing PEG-DA (60% v/v), photo-initiator (2% v/v), BCECF-dextran solution at 1 mg/mL concentration (10% v/v), and water (28% v/v). For the oxygen sensitive elements, the precursor solution was made by mixing PEG-DA (60% v/v), photo-initiator (2% v/v), ruthenium complex solution at 5 mg/mL concentration (2% v/v), and water (36% v/v). The concentration of each fluorophore was determined so the fluorophores would have similar fluorescence dynamic ranges under experimental conditions. The precursor solution was injected into each microchannel and cured by UV light that was projected through the photomask. The final sensor contained 2 arrays with 3 elements in each, allowing for measurement of two independent chemicals. The sensor was stored in 75%

ethyl alcohol for further experiments.

Cell Culture

Cell culture media was prepared with Dulbecco's modified Eagle's medium (DMEM) without phenol red supplemented with 4 mM L-glutamine, 1.5 g/L sodium bicarbonate, 4.5 g/L glucose, 200 U/mL penicillin, 200 μg/mL streptomycin and bovine calf serum 10%(v/v).

Fibroblast cells (NIH/3T3) were purchased from ATCC (Manassas, VA). The initial pH of the cell culture media was 7.4 and the cells were grown in a polystyrene tissue culture flask (75 cm^2 growth area) to desired quantity for the experiment. The cells were subcultured using the following procedure.

1. Remove all media in T-flask and add 5~10 mL of trypsin-EDTA
2. Incubate at 37 ^oC over 5 min. and check under the microscope for cell suspension
3. Add 10~15 ml of fresh media to dilute trypsin-EDTA
4. Move all media with cells into a 50mL centrifuge tube and centrifuge 5 min. at 1000 rpm
5. Remove all media and add 25 ml of fresh media into the centrifuge tube
6. Resuspend the cells with a vortex mixer (very slight touch required to avoid damage to the cells)
7. Count the number of cells with a hemocytometer

8. Aliquot into five 5 flasks, 5 mL each, and add 20 mL of fresh media to each flask
9. Check conditions of the cells under the microscope and incubate T-flask

During the cell culture, the temperature and CO_2 level were kept constant at 37 °C and 5 % by an incubator (NuAire, Plymouth, MN). When the cells were grown to the desired quantity, some of the cells were inoculated into the bioreactor and the others were frozen at –80 °C with complete growth medium supplemented with dimethyl sulfoxide (DMSO, 10% v/v).

Rotary Cell Culture System

The Synthecon (Houston, TX) Rotary Cell Culture System (RCCS) was used for cell culturing. This bioreactor can be used in three modes including infusion, injection, and recirculation. For this research, the infusion mode was used for easy sampling. Figure 5.1 shows the picture of Synthecon RCCS bioreactor.

The bioreactor was designed to allow the continuous growth of three dimensional tissue and cells, permitting continuous perfusion of nutrients and removal of waste, thus avoiding the need for removal of the vessel to replenish the media. The cylindrical culture vessel rotates about the horizontal axis to suspend the cells in the media. The core filter (3~5 μm mesh size) kept the cells inside the vessel and rotates at the same speed as the outer vessel to generate laminar flow inside of the vessel. A bubble trap removes air bubbles in the vessel that may cause cell death due to high shear stress. As the cells grow in size, the rotation speed is adjusted to compensate for the increased settling rates of the larger particles. Oxygen supply and carbon dioxide removal is

achieved through a gas permeable silicon rubber membrane. A fan is positioned to increase air flow around the silicon membrane housing. Suspension cells can be loaded into the vessel directly and anchorage dependent cells can be loaded with a microcarrier, which is a small and beaded material made of silica, glass, dextran or similar material. Unlike cell and tissue cultures grown in two-dimensional flat systems, cell and tissue cultures grown in the RCCS are functionally similar to tissues in a human body which enables three-dimensional culture *in vitro* that mimic the structure and function of the same tissue *in vivo*.

Bioreactor Setup

The entire system was sterilized before addition of cell culture media and cell inoculation. Only certain components in the RCCS can be sterilized by autoclaving since it has several electronic parts. The autoclavable components include the rotating wall vessel, shaft, screw, oxygenator, bubble trap, flow cell, cap, fitting, tubing, tube connector, core filter, valve, media reservoir, and waste reservoir. An autoclave condition of 20 minutes at 120 ^{o}C was used as recommended by the manufacturer.

All of the components to be autoclaved, including a quartz flow cell which is used as the sensor holder, were filled with 75% ethyl alcohol for 24 hours and then rinsed with deionized water and cleaned before autoclaving. The components were disassembled, wrapped with aluminum foil, and placed inside of autoclave. Each tubing was numbered with autoclaving indicating tape for easy and fast assembly. After autoclaving, all of the components were exposed to UV light for 24 hours in a laminar

flow bench to ensure sterile conditions. The entire system was reassembled in a laminar flow bench in reverse order of the disassembly.

After autoclaving and reassembly, the RCCS was filled with the cell culture media. A media reservoir was first filled with fresh cell culture media. Media was fed to the bubble trap by running the peristaltic pump at high speed. When the media was filled in the bubble trap at approximately 2/3 of its total volume, the outlet of vessel was locked and the inlet was opened. The pump was re-run to fill the rotating wall vessel with media. When the rotating wall vessel was almost full, microcarrier (autoclaved in a 0.1M PBS solution prior to use) and cells were inoculated through injection ports on the side of the rotating wall vessel. Initial cell concentration was 3.1×10^5 cells/mL and microcarrier concentration was 3 g/L (dry weight). In this step, many of the bubbles were generated inside of the vessel because serum inside of cell culture media has high viscosity. After all bubbles were removed naturally, the vessel was completely filled with cell culture media by tilting the vessel and refilling the media. After coupling to the flow cell with the microarray sensor, the reactor and imaging system were placed in an incubator. The entire procedure was performed in a laminar flow bench.

Calibration Dataset

Calibration data were acquired off-line before cell inoculation using the same cell culture media used in the RCCS. In short, cell culture media was placed into a beaker and a pH meter (Thermo, Waltham, MA) and a standard Clark electrode oxygen sensor (MI-730, Microelectrodes, Bedford, NH) were used to externally monitor pH and

O_2. The commercial oxygen sensor was calibrated at the start of the experiment using two water standards: nitrogen gas (0% O_2) and air (21% O_2). The commercial pH meter was calibrated with standard buffer solutions. The fifteen spiked values were generated for pH (5.7~7.7) and dissolved oxygen (0~21%) with a random number generator in Matlab (Mathworks, Natick, MA). The concentration of each analyte is presented in Table 5.1. To build a calibration model, pH and dissolved oxygen were changed by adding HCl or NaOH solutions and bubbling air or N_2 in the solution to have the desired pH and dissolved oxygen values shown in Table 5.1. The fluorescence image was captured (2 sec. exposure) and readings from the pH/oxygen electrode sensor were recorded. All images were imported to a PC for further analysis.

Prediction Dataset

A schematic diagram for the cell culture experiment is shown in Figure 5.2. The rotating wall vessel and the core filter were kept rotating at 10 rpm as recommended by the manufacturer. The pumping speed of the peristaltic pump was adjusted to have 2 mL/min flow rate as recommended by the manufacturer. The cell culture media was circulated through the rotating wall vessel, flow cell, valves, bubble trap, and oxygenator by the pump. The fluorescence image of the sensor was captured using previously developed imaging system in the same manner as the calibration step. For the sample collection, 3-way valves were manipulated for injection of fresh cell culture media and ejection of old cell culture media. The reactor sampling port, commercial pH probe, and commercial oxygen probe were placed in a 15mL centrifuge tube. The tube was filled

with cell culture media up to 10 mL and each probe reading was recorded. Those two procedures were performed five times per day over two weeks as follows: right before media refreshing (media refreshing was performed every 24 hours by injecting 200 mL of fresh media to increase pH over 7.0), 1 hour after media refreshing, 3 hours after media refreshing, 6 hours after media refreshing, and 12 hours after media refreshing. Oxygenation of the RCCS is normally maintained at a constant dissolved oxygen level in the cell culture media. Thus, it was expected that the sensor response to oxygen will be a flat line over the experimental period. In order to test the sensor with greater dynamic range, oxygenation was intentionally stopped for the three hours between three hours after media refreshing and six hours after media refreshing. This was performed by stopping the peristaltic pump and oxygenator fan. The standard error of calibration (SEC) and the standard error of prediction (SEP) were calculated in the same manner as described in the previous chapter.

Results and Discussion

Calibration Dataset

Unlike glucose free cell culture media which is used in CHAPTER IV, actual cell culture media has a high glucose concentration (4.5 g/L). Glucose is the best nutrient for growth of cells, bacteria, and fungus. Since the experimental setup was open to the air, severe contamination was observed during the calibration data collection. In order to overcome that problem, excessive antibiotics and fungizone were added in the cell culture media (10 times higher concentration than regular cell culture media).

In order to build calibration models for pH and O_2, 15 spiked sample images were collected. As shown in Figures 5.3 and 5.4, the microarray sensor shows good sensitivity and specificity. Within the tested pH range, 3rd order polynomial fitting successfully traced the pH sensor response (R=0.9954). Linear regression was applied to build the oxygen calibration model which agrees with the Stern-Volmer quenching model at low concentration (R=0.9985).

Prediction Dataset

In order to test the feasibility of the microarray sensor for use in bioprocess monitoring, the sensor and imaging system was coupled to a bioreactor and tested over two weeks. The sensor image was collected 5 times per day and analyte concentration was predicted based on the calibration model that was acquired in the previous section.

Figure 5.5 shows a plot of pH prediction and pH measured by a commercial probe sensor. The result clearly shows that the sensor response is reliable for monitoring pH in the cell culture media. In a 24 hours period, the pH of media decreased as nutrients were taken up by the cells and as the levels of respiratory by-products (mostly acidic) increased. The pH of the media goes back up to the optimal range by media refreshing every 24 hours. Figure 5.6 shows a plot of pH measured by a commercial sensor versus pH predicted by the microarray sensor. The result shows that the sensor was able to monitor pH of cell culture media on-line for over two weeks with minimal bias or drift.

Figure 5.7 shows a plot of O_2 prediction and O_2 measured by a commercial probe sensor. The result shows that the sensor response is reliable for monitoring

dissolved oxygen in the cell culture media. For the cell proliferation, oxygen in cell culture media is consumed by respiratory activity of the cells. An oxygenator was used in this bioreactor to maintain oxygen level as well as carbon dioxide level. However, the oxygenation was stopped for 3 hours per day to verify the sensor's dynamic range. As shown in Figure 5.7, the O_2 level dropped below 13 % when oxygenation stopped, and the sensor was able to sense the change in dissolved oxygen level. The O_2 level of the media goes back up to the optimal range by re-running the circulation and oxygenation. Figure 5.8 shows a plot of O_2 measured by a commercial sensor versus O_2 predicted by the microarray sensor. The results show that the sensor was able to monitor the dissolved oxygen level of cell culture media on-line for over two weeks.

Conclusion

This chapter serves as a culmination of the previous chapters in bringing together all facets of the project into a single experiment that mimics the final application of this project. The sensing system and array were added to an existing rotary cell culturing system and cells were cultured and monitored. The normal fluctuations of both pH and oxygen were monitored using both commercial sensing assays and the micro-array sensing system. The results contained more error and anomalies than in the *in vitro* experiments. The SEC and SEP for the pH sensor was 0.06 and 0.09, and for the oxygen sensor was 0.55 and 0.72. For both analytes, there was no significant degradation or drifting observed over two weeks. The results from this experiment proved feasibility of the proposed approach and confirmed that this methodology for automated cell

culturing is viable.

CHAPTER VI

CONCLUSION

This work has described the development of a multi-analyte sensitive hydrogel microarray sensor via microfluidic patterning of hydrogel structures to monitor pH and dissolved oxygen concentration simultaneously in cell culture media. It also described the development of an optical imaging system to quantify analyte concentration based on fluorescence intensity of the sensor. Highly cross-linked PEG hydrogels were fabricated using UV induced photopolymerization of acrylated PEGs. These hydrogels are hydrophobic, optically transparent, and easily manipulated. In addition, they are able to anchor to glass slides and easily encapsulate functional agents that give the potential to be used as biosensors. BCECF-dextran and ruthenium complex were used as sensing agents and immobilized into the hydrogel structures. A series of tests for sensitivity, stability, reversibility, and temporal/spatial uniformity were performed and revealed the feasibility for use in biosensing applications. The sensor was viable after sterilization with ethanol, proving it can be used in bioprocess monitoring without introducing contamination.

A compact and inexpensive optical system was developed to capture the fluorescence image of the hydrogel microarray sensor with a blue LED, a series of optical filters and lenses, a quartz flow cell and a monochrome CCD camera. All these components are commercially available and inexpensive compared to complicated microscopic imaging systems. The imaging system is sufficiently reliable for this application and its compact size enables operation inside of a typical incubator. The

sensor and the imaging system was combined and introduced into a bioreactor for two weeks of fibroblast cultivation. It was established that the sensor was capable of measuring pH and dissolved oxygen during a typical bioprocess in cell culture media across the biological range required for mammalian cell culture. The hydrogel based sensor is non-intrusive after placement inside the bioprocess system, has a simple and highly reproducible manufacturing method, and has a response time adequate for cell culture monitoring.

The results presented in this study suggest that this technique can be easily extended to introduce more sensing agents, allowing for a complete lab-on-a-chip technology for cell culture monitoring. Further research would include making microarrays with sensing agents capable of detecting glucose, lactate, and nitric oxide. In addition to the introduction of more sensing agents, miniaturization of the sensor chip and optical system would allow for an inexpensive modulated portable monitoring system capable of disposable implementation for cell culturing systems.

REFERENCES

[1] Q. T. Trinh, G. Gerlach, J. Sorber, and K. F. Arndt, "Hydrogel-based piezoresistive pH sensors: design, simulation and output characteristics," *Sensors and Actuators B*, **117**, 17-26 (2006).

[2] J. Samuel, A. Strinkovski, K. Lieberman, M. Ottolenghi, D. Avnir, and A. Lewis, "Miniaturization of organically doped sol-gel materials - a microns-size fluorescent pH sensor," *Materials Letters*, **21**, 431-434 (1994).

[3] U. Narang, R. Gvishi, F. V. Bright, and P. N. Prasad, "Sol-gel-derived micron scale optical fibers for chemical sensing," *Journal of Sol-Gel Science and Technology*, **6**, 113-119 (1996).

[4] J. Lin, "Recent development and applications of optical and fiber-optic pH sensors," *Trends in Analytical Chemistry*, **19**, 541-552 (2000).

[5] P. Hartmann, M. Leiner, and M. E. Lippitsch, "Response characteristics of luminescent oxygen sensors," *Sensors and Actuators B*, **29**, 251-257 (1995).

[6] C. Mcdonagh, C. Kolle, A. K. Mcevoy, D. L. Dowling, A. A. Cafolla, S. J. Cullen, and B. D. Maccraith, "Phase fluorometric dissolved oxygen sensor," *Sensors and Actuators B*, **74**, 124-130 (2001).

[7] R. G. Harrison, *Organization and Development of the Embryo*, Garland, New York (1988).

[8] P. Doran, "Foreign protein production in plant tissue cultures," *Current Opinion in Biotechnology*, **11**, 199-204 (2000).

[9] C. Holmes, "Novel peptide-based biomaterial scaffolds for tissue engineering," *Trends in Biotechnology*, **20**, 16-21 (2002).

[10] L. Jackson, L. Trudel, J. Fox, and N. Lipman, "Evaluation of hollow fiber bioreactors as an alternative to murine ascites production for small scale monoclonal antibody production," *Journal of Immunological Methods*, **189**, 217-231 (1996).

[11] K. Schugerl, "Progress in monitoring, modeling and control of bioprocesses during the last 20 years," *Journal of Biotechnology*, **85**, 149-173 (2001).

[12] M. Nomi, A. Atala, P. Coppi, and S. Soker, "Principals of neovascularization for tissue engineering," *Molecular Aspects of Medicine*, **23**, 463-483 (2002).

[13] United Network for Organ Sharing, Current Organ Donor Data, Available: www.unos.org, August 1 (2006).

[14] U.S. Department of Health and Human Services: Health Resources and Services Administration, Available: www.hrsa.gov, August 1 (2006).

[15] H. Graf, "Manufacturing and supply of monovalent oral polio vaccines," *Biologicals*, **34**, 141-144 (2006).

[16] K. Trabelsi, S. Rourou, and H. Loukil, "Optimization of virus yield as a strategy to improve rabies vaccine production by vero cells in a bioreactor," *Journal of Biotechnology*, **121**, 261-271 (2006).

[17] A. Mayr, "Development of a non-immunising, paraspecific vaccine from attenuated pox viruses: a new type of vaccine," *New Microbiologica*, **26**, 7-12 (2003).

[18] R. Rajkannan, M. D. Dhanaraju, and D. Gopinath, "Development of hepatitis b oral vaccine using b-cell epitope loaded plg microparticles," *Vaccine*, **24**, 5149-5157 (2006).

[19] R. P. Singh, S. K. Bandyopadhyay, and B. P. Sreenivasa, "Production and characterization of monoclonal antibodies to peste des petits ruminants (PPR) virus," *Veterinary Research Communications,* **28**, 623-639 (2004).

[20] A. D. Wilson, L. Harwood, and S. Torsteinsdottir, "Production of monoclonal antibodies specific for native equine IgE and their application to monitor total serum IgE responses in icelandic and non-icelandic horses with insect bite dermal hypersensitivity," *Veterinary Immunology and Immunopathology*, **112**, 156-170 (2006).

[21] Z. Vajo, and W. C. Duckworth, "Genetically engineered insulin analogs: diabetes in the new millennium," *Pharmacological Reviews*, **52**, 1-9 (2000).

[22] S. Choe, "Brassinosteroid biosynthesis and inactivation," *Physiologia Plantarum*, **126**, 539-548 (2006).

[23] M. Butler, *Animal Cell Culture and Technology: Principles and Products*, Taylor and Francis, New York (1984).

[24] R. Mitteregger, G. Vogt, E. Rossmanith, and D. Falkenhagen, "Rotary cell culture system (RCCS): a new method for cultivating hepatocytes on microcarriers," *International Journal of Artificial Organs*, **22**, 816-822 (1999).

[25] S. W. Huang, “Effect of pH on high-temperature production of bacterial penicillin acylase in *escherichia coli*,” *Biotechnology Progress*, **18**, 668-671 (2002).

[26] R. J. Rowbury, and M. Goodson, “An extracellular acid stress-sensing protein needed for acid tolerance induction in *escherichia coli*,” *FEMS Microbiology Letters*, **174**, 49-55 (1999).

[27] R. I. Fresheny, *Culture of Animal Cells: A Manual of Basic Technique*, Wiley-Liss, New York (2000).

[28] S. D. Patel, “The lactate issue revisited: novel feeding protocols to examine inhibition of cell proliferation and glucose metabolism in hematopoietic cell cultures,” *Biotechnology Progress*, **16**, 885-892 (2000).

[29] S. Pazicni, “The redox behavior of the heme in cystathionine beta-synthase is sensitive to pH,” *Biochemistry*, **43**, 14684-14695 (2004).

[30] P. Vats, D. K. Sahoo, and U. C. Banerjee, “Production of phytase (myo-inositolhexakisphosphate phosphohydrolase) by Aspergillus niger van Teighem in laboratory-scale fermenter,” *Biotechnology Progress*, **20**, 737-743 (2004).

[31] D. Mattanovich, “Stress in recombinant protein producing yeasts,” *Journal of Biotechnology*, **113**, 121-135 (2004).

[32] R. J. Gillies, “A review of pH measurement methods and applications in cancers,” *IEEE Engineering in Medicine and Biology Magazine*, **23**, 57-64 (2004).

[33] Y. Chisti, “Build better industrial bioreactors,” *Chemical Engineering Progress*, **88**, 55-58 (1992).

[34] E. Martin, A. Pardo, and M. S. Guijarro, “Photophysics properties of fluorescein in alcoholic medium for different pH,” *Journal of Molecular Structure*, **142**, 197-200 (1986).

[35] K. Grattan, and G. E. Badini, “Use of sol-gel techniques for fiberoptic sensor applications,” *Sensors and Actuators A*, **26**, 483-487 (1991).

[36] J. R. Lakowicz, F. N. Castellano, and J. D. Dattelbaum, “Low frequency modulation sensors using nanosecond fluorophores,” *Analytical Chemistry*, **70**, 5115-5121, (1998).

[37] Y. Takahashi, and R. Shimada, “Coumarin-4-doped sol-gel coating film as optical pH sensor,” *Japanese Journal of Applied Physics Part 2*, **34**, 1594-1596 (1995).

[38] M. D. Sotomayor, M. A. Depaoli, and W. A. Deoliveira, “Fiber-optic pH sensor based on poly(o-methoxyaniline),” *Analytica Chimica Acta*, **353**, 275-280 (1997).

[39] Y. N. Shi, C. J. Seliskar, and W. R. Heineman, “Dual-analyte spectroscopic sensing in sol-gel derived polyelectrolyte-silica composite thin films,” *Talanta*, **47**, 1071-1076 (1998).

[40] P. S. Blank and H. S. Silverman, “pH measurement in single cardiac myocytes with SNARF-1,” *Biophysical Journal*, **57**, A137 (1990).

[41] H. Szmacinski and J. R. Lakowicz, "Optical measurements of pH using fluorescence lifetimes and phase-modulation fluorometry," *Analytical Chemistry*, **65**, 1668-1674 (1993).

[42] J. Lin and D. Liu, "An optical pH sensor with a linear response over a broad range," *Analytica Chimica Acta*, **408**, 49-55 (2000).

[43] S. Lee, B. L. Ibey, M. V. Pishko, and G. L. Coté, "Hydrogel microarray for monitoring of pH and dissolved oxygen in cell culture media," *Proceedings of the SPIE*, **6094**, 9-15 (2006).

[44] R. P. Haugland, *Handbook of Fluorescent Probes and Research Products*, Molecular Probes Inc., Carlsbad, CA (2002).

[45] L. C. Clark and L. M. Bargeron, "Left-to-right shunt detection by an intravascular electrode with hydrogen as an indicator," *Science*, **130**, 709-710 (1959).

[46] I. Bergman, "Rapid-response atmospheric oxygen monitor based on fluorescence quenching," *Nature*, **218**, 396 (1968).

[47] D. W. Lubbers and N. Opitz, "pO_2-optode, a new tool to measure pO_2 of biological gases and fluids by quantitative fluorescence photometry," *European Journal of Physiology*, **359**, 145 (1975).

[48] F. Baldini, M. Bacci, F. Cosi, and A. Delbianco, "Absorption-based optical-fiber oxygen sensor," *Sensors and Actuators B*, **7**, 752-757 (1992).

[49] H. W. Kroneis and H. J. Marsoner, "A fluorescence-based sterilizable oxygen probe for use in bioreactors," *Sensors and Actuators*, **4**, 587-592 (1983).

[50] I. S. Longmuir and J. A. Knopp, “Measurement of tissue oxygen with a fluorescent-probe,” *Journal of Applied Physiology*, **41**, 598-602 (1976).

[51] A. Sharma and O. S. Wolfbeis, “Fiberoptic oxygen sensor based on fluorescence quenching and energy-transfer,” *Applied Spectroscopy*, **42**, 1009-1011 (1988).

[52] O. S. Wolfbeis, M. Leiner, and H. E. Posch, “A new sensing material for optical oxygen measurement, with the indicator embedded in an aqueous phase,” *Mikrochimica Acta*, **3**, 359-366 (1986).

[53] I. Klimant and O. S, Wolfbeis, “Oxygen-sensitive luminescent materials based on silicone-soluble ruthenium diimine complexes,” *Analytical Chemistry*, **67**, 3160-3166 (1995).

[54] X. M. Li, F. C. Ruan, and K. Y. Wong, “Optical characteristics of a ruthenium(II) complex immobilized in a silicone-rubber film for oxygen measurement,” *Analyst*, **118**, 289-292 (1993).

[55] J. F. Gouin, F. Baros, and D. Birot, “A fibre-optic oxygen sensor for oceanography,” *Sensors and Actuators B*, **39**, 401-406 (1997).

[56] M. F. Choi and X. Dan, “Single standard calibration for an optical oxygen sensor based on luminescence quenching of a ruthenium complex,” *Analytica Chimica Acta*, **403**, 57-65 (2000).

[57] W. Wang, C. E. Reimers, and S. C. Wainright, “Applying fiber-optic sensors for monitoring dissolved oxygen,” *Sea Technology*, **40**, 69 (1999).

[58] C. Malins, M. Niggemann, and B. D. Maccraith, "Multi-analyte optical chemical sensor employing a plastic substrate," *Measurement Science & Technology*, **11**, 1105-1110 (2000).

[59] C. M. Ingersoll and F. V. Bright, "Using sol-gel-based platforms for chemical sensors," *Chemtech*, **27**, 26-31 (1997).

[60] B. D. Maccraith, G. Okeeffe, and C. Mcdonagh, "LED-based fiber optic oxygen sensor using sol-gel coating," *Electronics Letters*, **30**, 888-889 (1994).

[61] T. Miyashita and J. F. Chen, "Fabrication of polymer organized thin films containing ruthenium complexes," *Polymer Journal*, **31**, 1121-1126 (1999).

[62] C. Preininger, I. Klimant, and O. S. Wolfbeis, "Optical-fiber sensor for biological oxygen-demand," *Analytical Chemistry*, **66**, 1841-1846 (1994).

[63] K. P. Mcnamara, X. P. Li, A. D. Stull, "Fiber-optic oxygen sensor based on the fluorescence quenching of tris (5-acrylamido, 1,10 phenanthroline) ruthenium chloride," *Analytica Chimica Acta*, **361**, 73-83 (1998).

[64] E. Singer, G. L. Duveneck, and M. Ehrat, "Fiber optic sensor for oxygen determination in liquids," *Sensors and Actuators A*, **42**, 542-546 (1994).

[65] D. J. Stufkens, A. Oskam, and M. W. Kokkes, "Metal-ligand charge-transfer photochemistry - metal metal bonded complexes," *ACS Symposium Series*, **307**, 66-84 (1986).

[66] B. H. Weigl, A. Holobar, Trettnak W, Et Al. "Optical triple sensor for measuring ph, oxygen and carbon-dioxide," *Journal of Biotechnology*, **32**, 127-138 (1994).

[67] D. Kieslinger, S. Draxler, and K. Trznadel, "Lifetime-based capillary waveguide sensor instrumentation," *Sensors and Actuators B*, **39**, 300-304 (1997).

[68] H. Chuang and M. A. Arnold, "Radioluminescent light source for optical oxygen sensors," *Analytical Chemistry*, **69**, 1899-1903 (1997).

[69] S. J. Sofia and E. Merill, *Poly(ethylene glycol): Chemistry and Biological Applications*, American Chemical Society, Washington D.C. (1997).

[70] P. D. Drumheller and J. A. Hubbell, "Densely cross-linked polymer networks of poly(ethylene glycol) in trimethylolpropane triacrylate for cell-adhesion-resistant surfaces," *Journal of Biomedical Materials Research*, **29**, 207-215 (1995).

[71] J. Lee, P. A. Martic, and J. S. Tan, "Protein adsorption on pluronic copolymer-coated polystyrene particles," *Journal of Colloid and Interface Science*, **131**, 252-266 (1989).

[72] J. H. Lee, B. J. Jeong, and H. B. Lee, "Plasma protein adsorption and platelet adhesion onto comb-like PEO gradient surfaces," *Journal of Biomedical Materials Research*, **34**, 105-114 (1997).

[73] K. D. Park, Y. S. Kim, D. K. Han, Y. H. Kim, E. H. Lee, H. Suh, and K. S. Choi, "Bacterial adhesion on PEG modified polyurethane surfaces," *Biomaterials*, **19**, 851-859 (1998).

[74] A. Razatos, Y. I. Ong, F. Boulay, D. L. Elbert, J. A. Hubbell, M. M. Sharma, and G. Georgiou, "Force measurements between bacteria and poly(ethylene glycol)-coated surfaces," *Langmuir*, **16**, 9155-9158 (2000).

[75] E. Tziampazis, J. Kohn, and P. V. Moghe, "PEG-variant biomaterials as selectively adhesive protein templates: model surfaces for controlled cell adhesion and migration," *Biomaterials*, **21**, 511-520 (2000).

[76] A. S. Sawhney, C. P. Pathak, and J. A. Hubbell, "Bioerodible hydrogels based on photopolymerized poly(ethylene glycol)-co-poly(alpha-hydroxy acid) diacrylate macromers," *Macromolecules*, **26**, 581-587 (1993).

[77] A. S. Sawhney, C. P. Pathak, J. J. Vanrensburg, R. C. Dunn, and J. A. Hubbell, "Optimization of photopolymerized bioerodible hydrogel properties for adhesion prevention," *Journal of Biomedical Materials Research*, **28**, 831-838 (1994).

[78] G. M. Cruise, D. S. Scharp, and J. A. Hubbell, "Characterization of permeability and network structure of interfacially photopolymerized poly(ethylene glycol) diacrylate hydrogels," *Biomaterials*, **19**, 1287-1294 (1998).

[79] R. J. Russell, A. C. Axel, K. L. Shields, and M. V. Pishko, "Mass transfer in rapidly photopolymerized poly(ethylene glycol) hydrogels used for chemical sensing," *Polymer*, **42**, 4893-4901 (2001).

[80] M. B. Mellott, K. Searcy, and M. V. Pishko, "Release of protein from highly cross-linked hydrogels of poly(ethylene glycol) diacrylate fabricated by uv polymerization," *Biomaterials*, **22**, 929-941 (2001).

[81] N. Bhattarai, H. R. Ramay, J. Gunn, F. A. Matsen, and M. Q. Zhang, "Peg-grafted chitosan as an injectable thermosensitive hydrogel for sustained protein release," *Journal of Controlled Release*, **103**, 609-624 (2005).

[82] B. Kim, “Synthesis of enzyme-containing PEG hydrogel nanospheres for optical biosensors,” *Polymer Korea*, **29**, 613-616 (2005).

[83] K. T. Nguyen and J. L. West, “Photopolymerizable hydrogels for tissue engineering applications,” *Biomaterials*, **23**, 4307-4314 (2002).

[84] S. R. Sheth and D. Leckband, “Measurements of attractive forces between proteins and end-grafted poly(ethylene glycol) chains,” *Proceedings Of The National Academy of Sciences of The United States of America*, **94**, 8399-8404 (1997).

[85] C. P. Quinn, M. V. Pishko, D. W. Schmidtke, M. Ishikawa, J. G. Wagner, P. Raskin, J. A. Hubbell, and A. Heller, “Kinetics of glucose delivery to subcutaneous tissue in rats measured with 0.3-mm amperometric microsensors,” *American Journal of Physiology-Endocrinology and Metabolism*, **269**, E155-E161 (1995).

[86] C. P. Quinn, C. P. Pathak, A. Heller, and J. A. Hubbell, “Photo-cross-linked copolymers of 2-hydroxyethyl methacrylate, poly(ethylene glycol) tetra-acrylate and ethylene dimethacrylate for improving biocompatibility of biosensors,” *Biomaterials*, **16**, 389-396 (1995).

[87] K. Sirkar and M. V. Pishko, “Amperometric biosensors based on oxidoreductases immobilized in photopolymerized poly(ethylene glycol) redox polymer hydrogels,” *Analytical Chemistry*, **70**, 2888-2894 (1998).

[88] C. P. Pathak, A. S. Sawhney, and J. A. Hubbell, "Rapid photopolymerization of immunoprotective gels in contact with cells and tissue," *Journal of The American Chemical Society*, **114**, 8311-8312 (1992).

[89] W. G. Koh, A. Revzin, and M. V. Pishko, "Poly(ethylene glycol) hydrogel microstructures encapsulating living cells," *Langmuir*, **18**, 2459-2462 (2002).

[90] R. J. Russell, M. V. Pishko, A. L. Simonian, and J. R. Wild, "Poly(ethylene glycol) hydrogel-encapsulated fluorophore-enzyme conjugates for direct detection of organophosphorus neurotoxins," *Analytical Chemistry*, **71**, 4909-4912 (1999).

[91] A. Revzin, R. J. Russell, V. K. Yadavalli, W. G. Koh, C. Deister, D. D. Hile, M. B. Mellott, and M. V. Pishko, "Fabrication of poly(ethylene glycol) hydrogel microstructures using photolithography," *Langmuir*, **17**, 5440-5447 (2001).

[92] A. Kumar and G. M. Whitesides, "Features of gold having micrometer to centimeter dimensions can be formed through a combination of stamping with an elastomeric stamp and an alkanethiol 'ink' followed by chemical etching," *Applied Physics Letters*, **63**, 2002-2004 (1993).

[93] S. Brittain, K. Paul, X. Zhao, and G. M. Whitesides, "Soft lithography and microfabrication," *Physics World*, **11**, 31-36 (1998).

[94] Y. Xia and G. M. Whitesides, "Soft lithography," *Annual Review of Material Science*, **28**, 153-184 (1998).

[95] N. Bowden, S. Brittain, A. G. Evans, J. W. Hutchinson, and G. M. Whitesides, "Spontaneous formation of ordered structures in thin films of metals supported on an elastomeric polymer," *Nature*, **393**, 146-149 (1998).

[96] E. J. Cho and F. V. Bright, "Pin-printed chemical sensor arrays for simultaneous multianalyte quantification," *Analytical Chemistry*, **74**, 1462-1466 (2002).

[97] K. Y. Vamsi, W. G. Koh, G. J. Lazur, and M. V. Pishko, "Microfabricated protein-containing poly(ethylene glycol) hydrogel arrays for biosensing," *Sensors and Actuators B*, **97**, 290–297 (2004).

[98] J. B. Brzoska, I. Benazouz, and F. Rondelez, "Silanization of solid substrates - a step toward reproducibility," *Langmuir*, **10**, 4367-4373 (1994).

[99] A. Folch, A. Ayon, O. Hurtado, M. A. Schmidt, and M. Toner, "Molding of deep polydimethylsiloxane microstructures for microfluidics and biological applications," *Journal of Biomechanical Engineering-Transactions of the ASME*, **121**, 28-34 (1999).

[100] A. Ulman, "Self-assembled monolayers of alkyltrichlorosilanes: building blocks for future organic materials," *Advanced Materials*, **2**, 573-582 (1990).

[101] R. Banga, J. Yarwood, A. M. Morgan, B. Evans, and J. Kells, "FTIR and AFM studies of the kinetics and self-assembly of alkyltrichlorosilanes and (perfluoroalkyl)trichlorosilanes onto glass and silicon," *Langmuir*, **11**, 4393-4399 (1995).

[102] T. J. Rink, R. Y. Tsien and T. Pozzan, "Cytoplasmic pH and free Mg2+ in lymphocytes," *The Journal of Cell Biology*, **95**, 189-196 (1982).

[103] H. Kautsky, “Quenching of luminescence by oxygen,” *Transactions of the Faraday Society*, **35**, 216-218 (1939).

[104] D. P. O'Neal, M. A. Meledeo, J. R. Davis, B. L. Ibey, V. A. Gant, M. V. Pishko, and G. L. Cote, “Oxygen sensor based on the fluorescence quenching of a ruthenium complex immobilized in a biocompatible poly(ethylene glycol) hydrogel,” *IEEE Sensors Journal*, **4**, 728-734 (2004).

[105] D. Willoughby, R. C. Thomas, and C. J. Schwiening, “Comparison of simultaneous pH measurements made with 8-hydroxypyrene-1,3,6-trisulphonic acid (HPTS) and pH-sensitive microelectrodes in snail neurons,” *Pflügers Archiv European Journal of. Physiology*, **436**, 615-622 (2004).

APPENDIX A

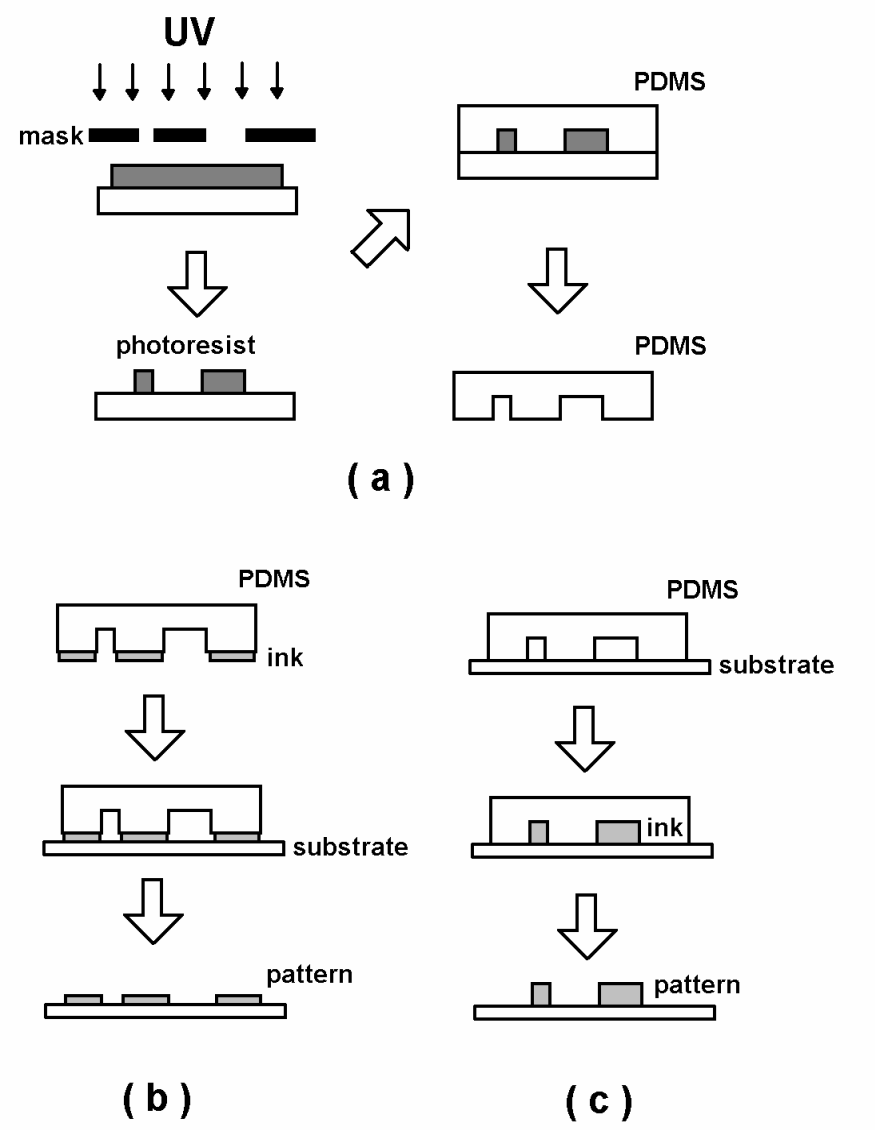

Figure 1.1. An illustration of soft lithography: (a) fabrication of a master and PDMS mold, (b) microcontact patterning, and (c) microfluidic patterning.

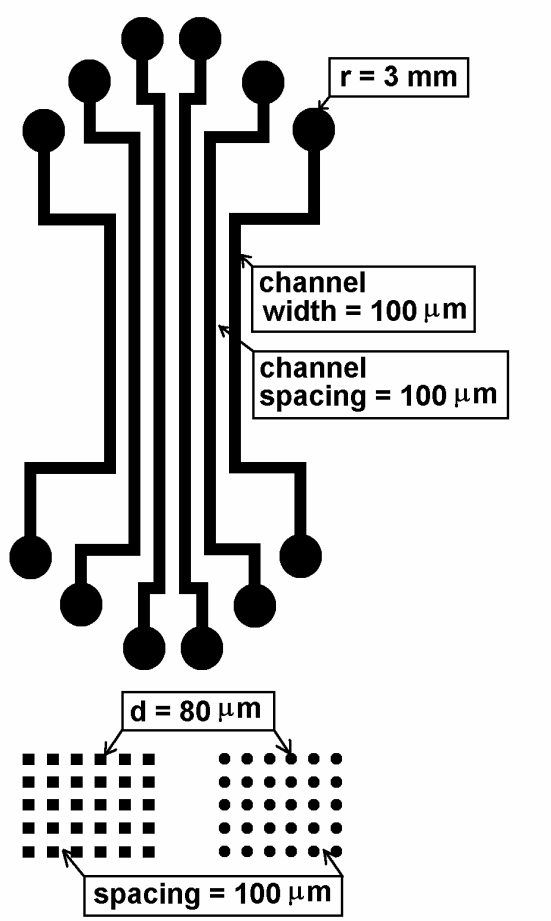

Figure 2.1. The photomask design for fabrication of master and microarray.

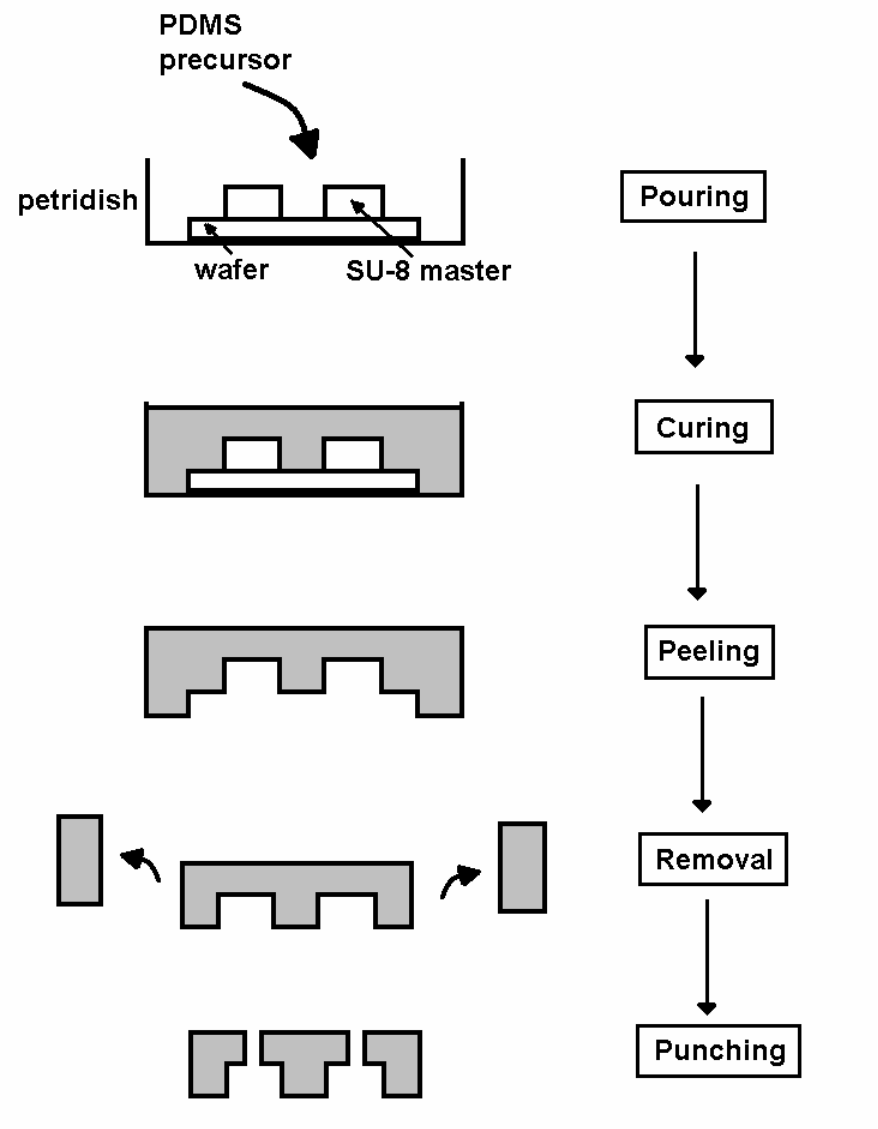

Figure 2.2. An illustration of PDMS fabrication procedure.

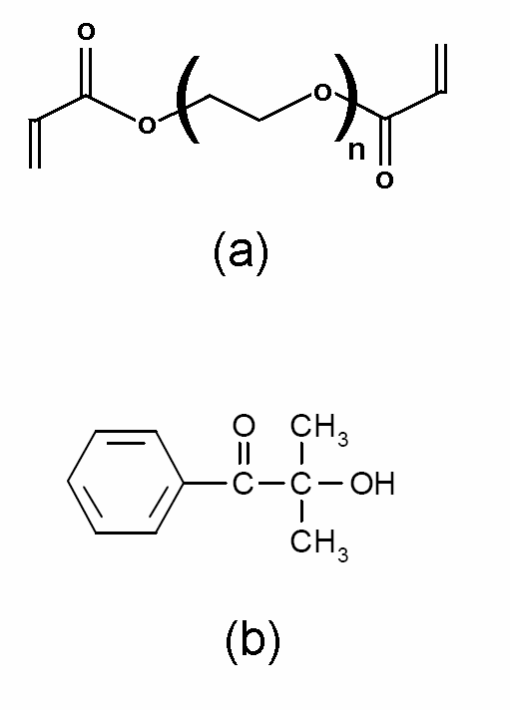

Figure 2.3. Chemical structures of PEG-DA (a) and photoinitiator Darocur® 1173 (b).

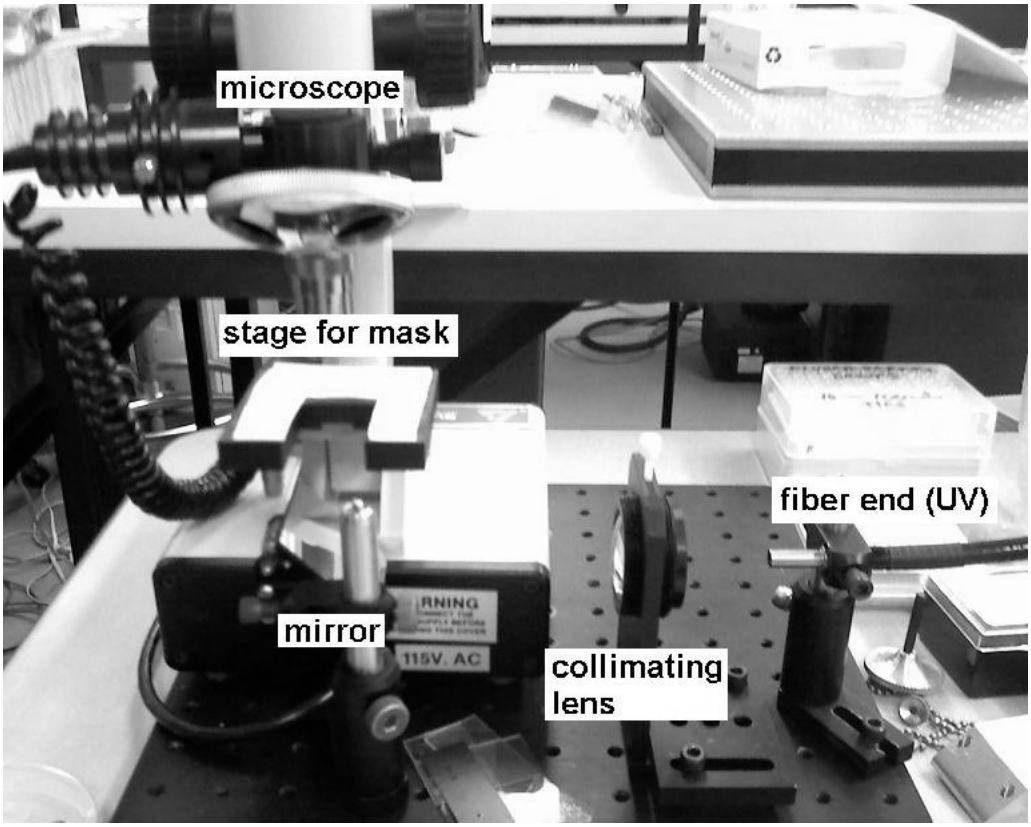

Figure 2.4. Modification of microscope to obtain collimated UV exposure.

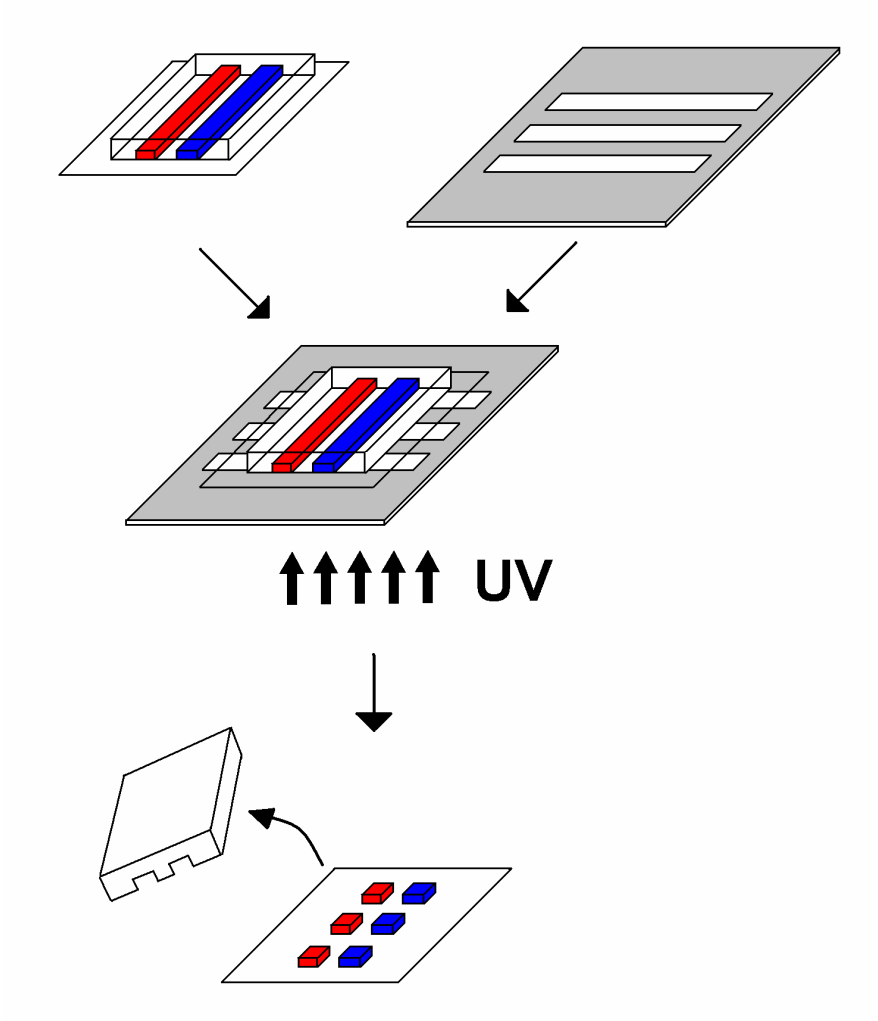

Figure 2.5. A scheme for fabrication of multi-analyte sensitive hydrogel microarray.

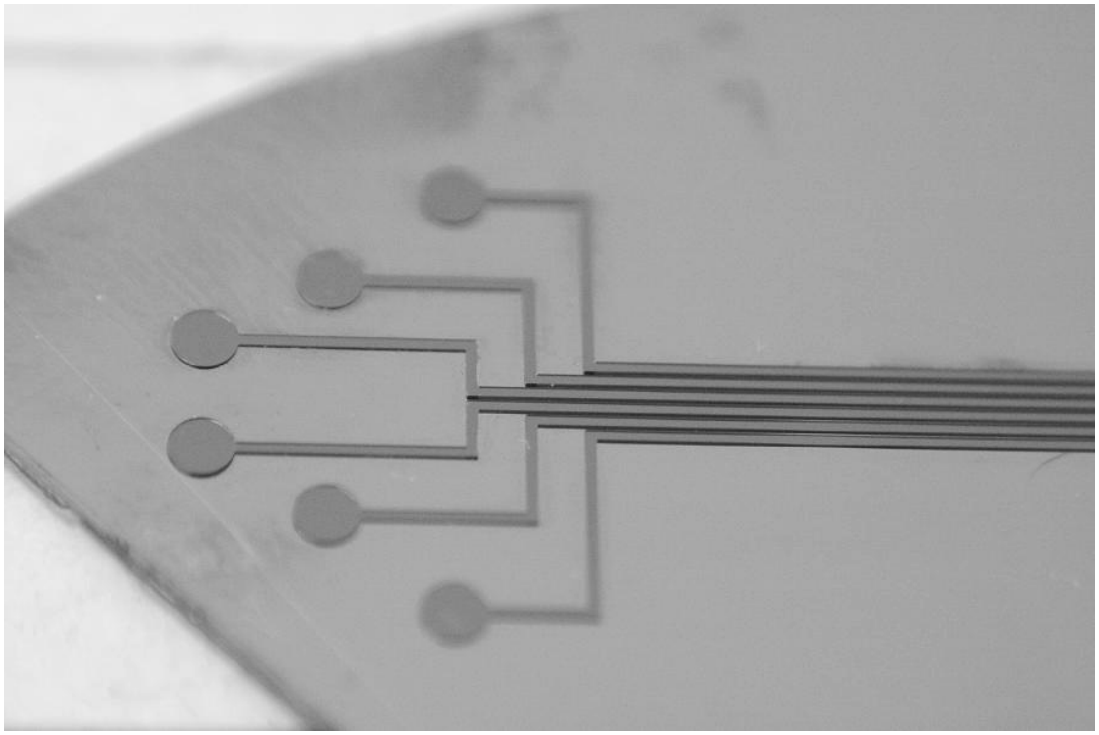

Figure 2.6. An example of SU-8 master on silicon wafer.

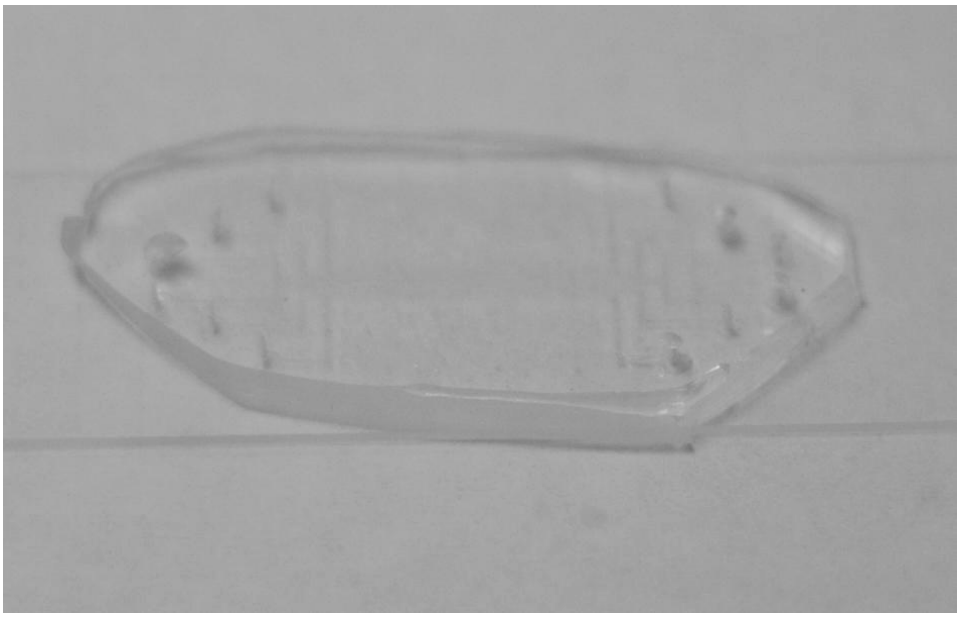

(a)

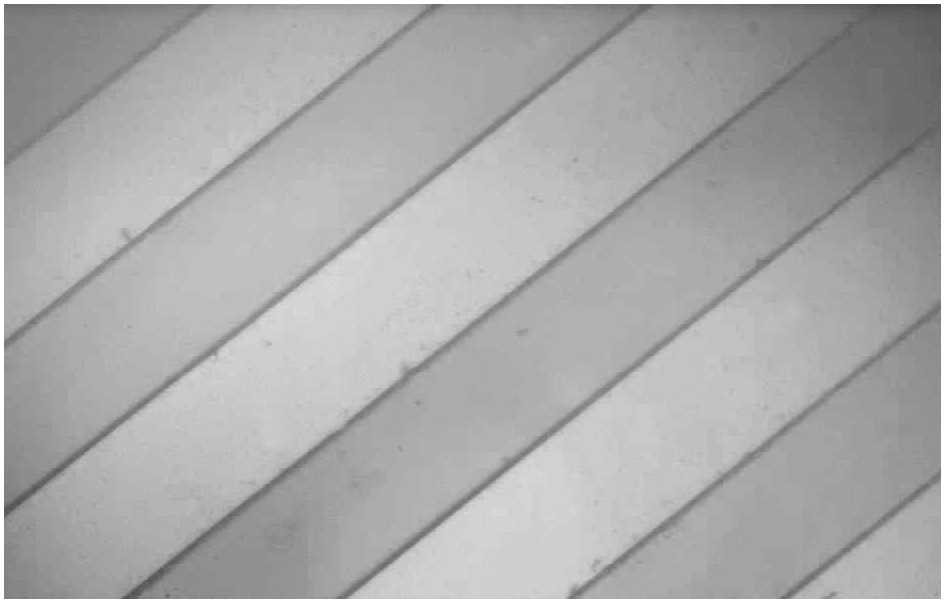

(b)

Figure 2.7. An example of a PDMS replica on a TPM modified glass slide (a) and a microscope image of microchannels on the PDMS (b).

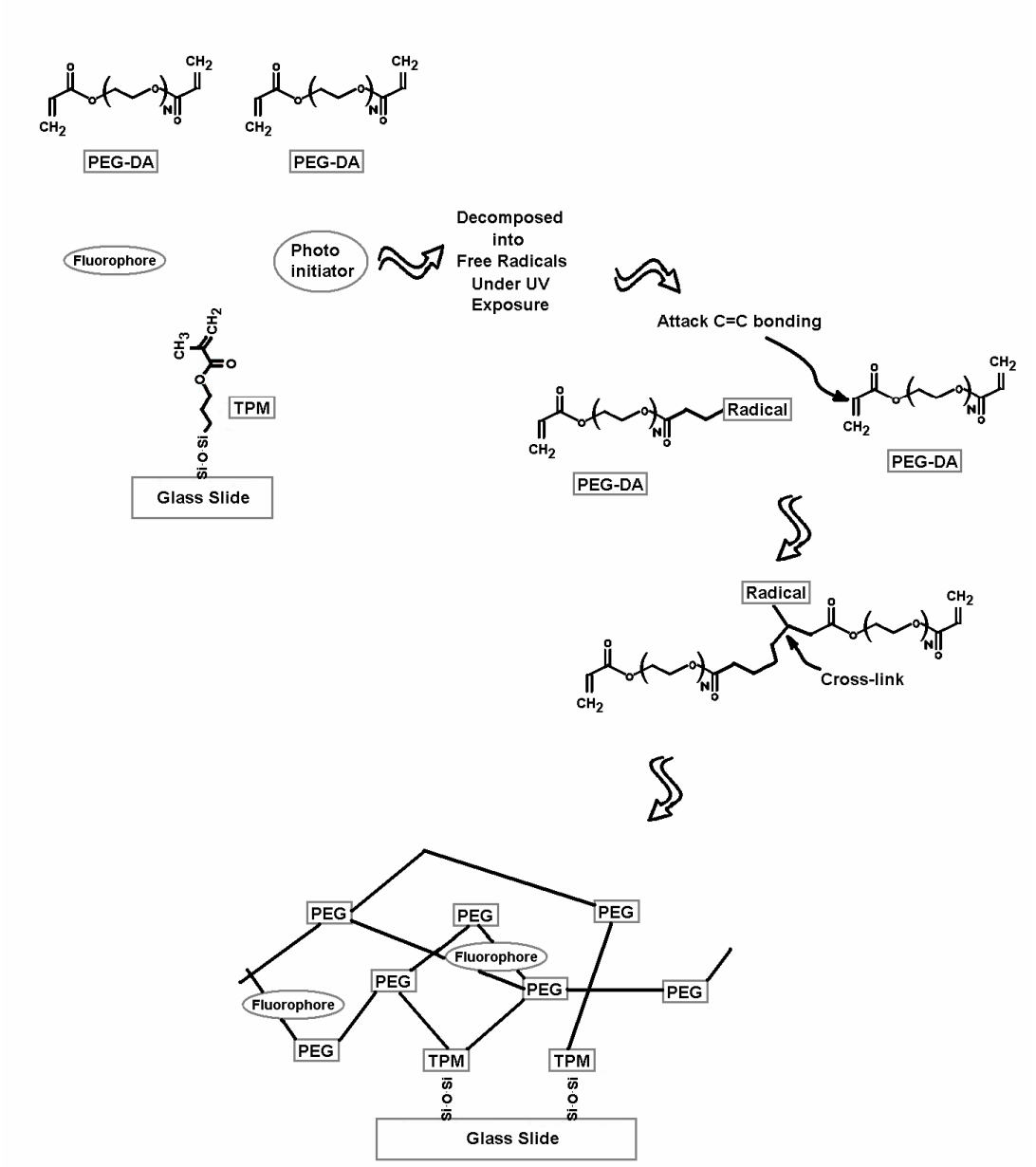

Figure 2.8. A scheme for chemical reactions during photopolymerization.

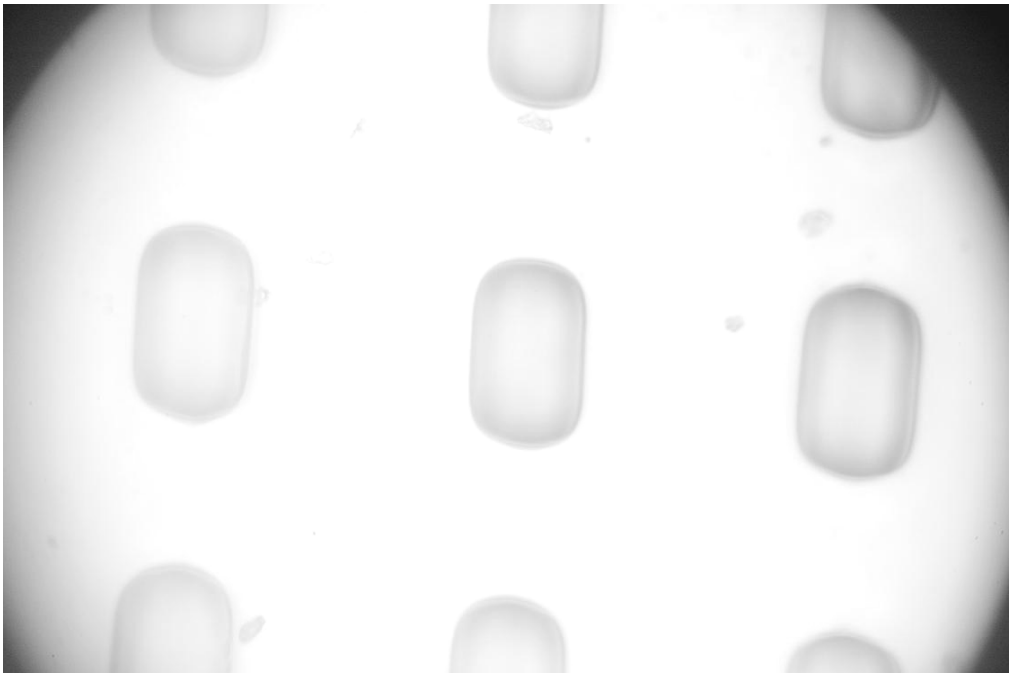

Figure 2.9. An example of a hydrogel microarray.

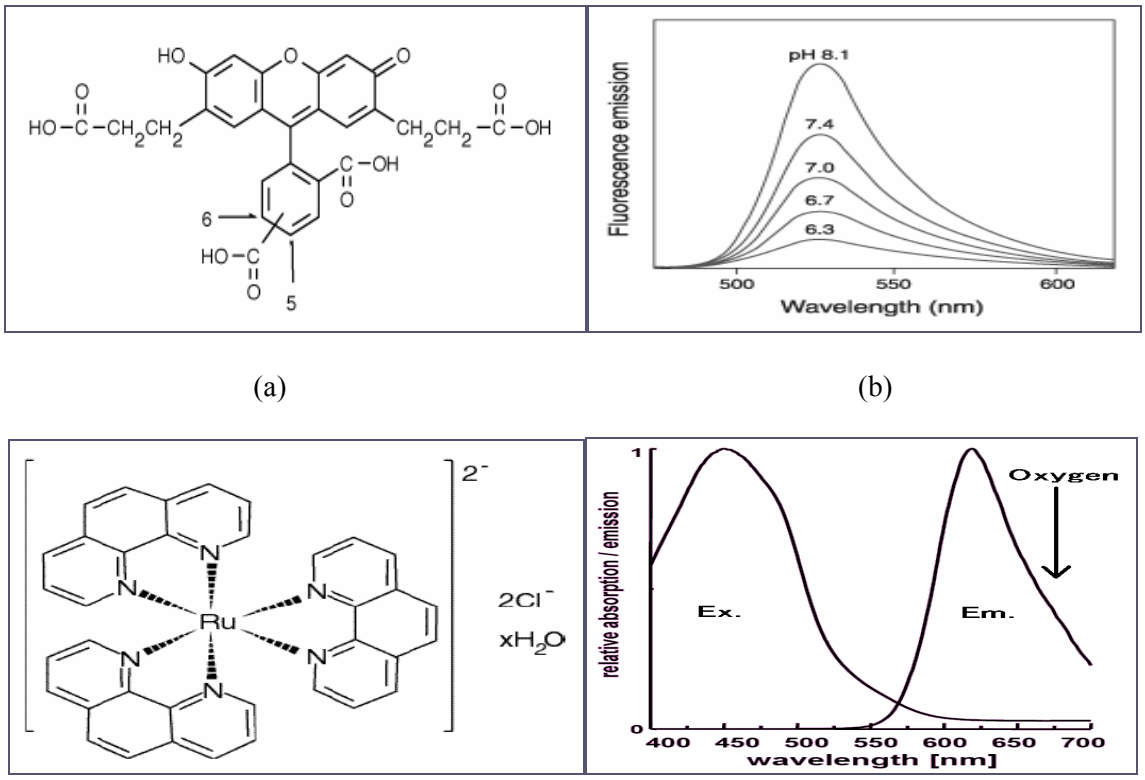

Figure 2.10. Chemical structure and fluorescence absorption/emission spectra for BCECF (a), (b) and Ruthenium complex (c), (d), respectively.

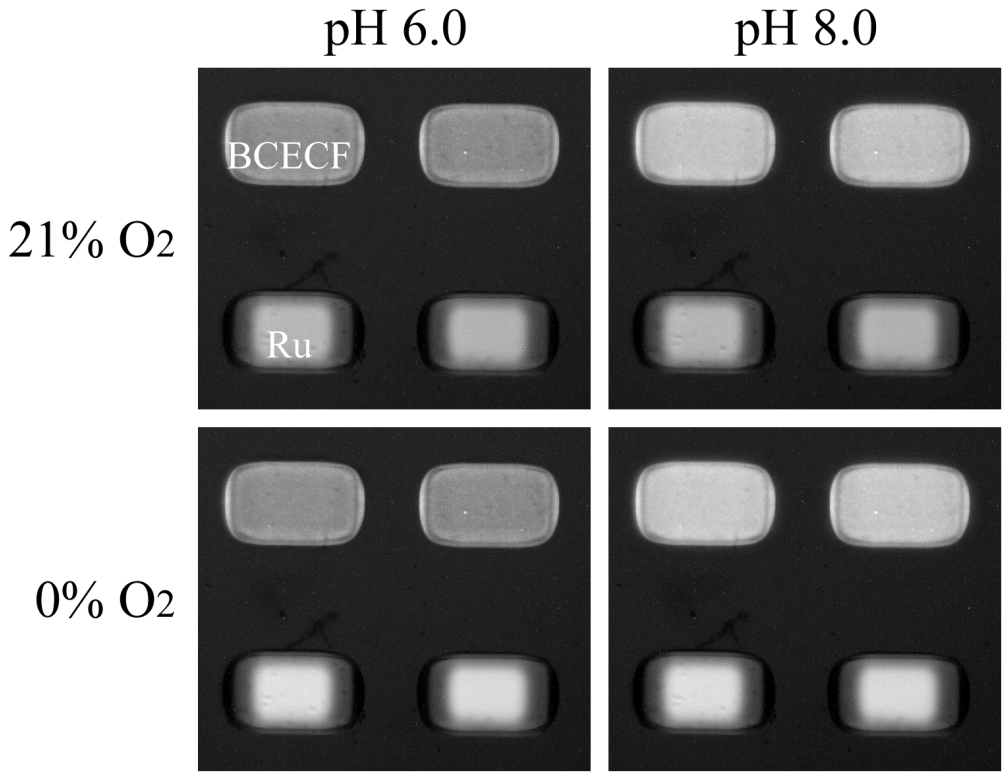

Figure 2.11. Fluorescence images of a multi-analyte sensitive hydrogel microarray in various sample solutions, BCECF immobilized element (upper) and ruthenium complex immobilized element (lower).

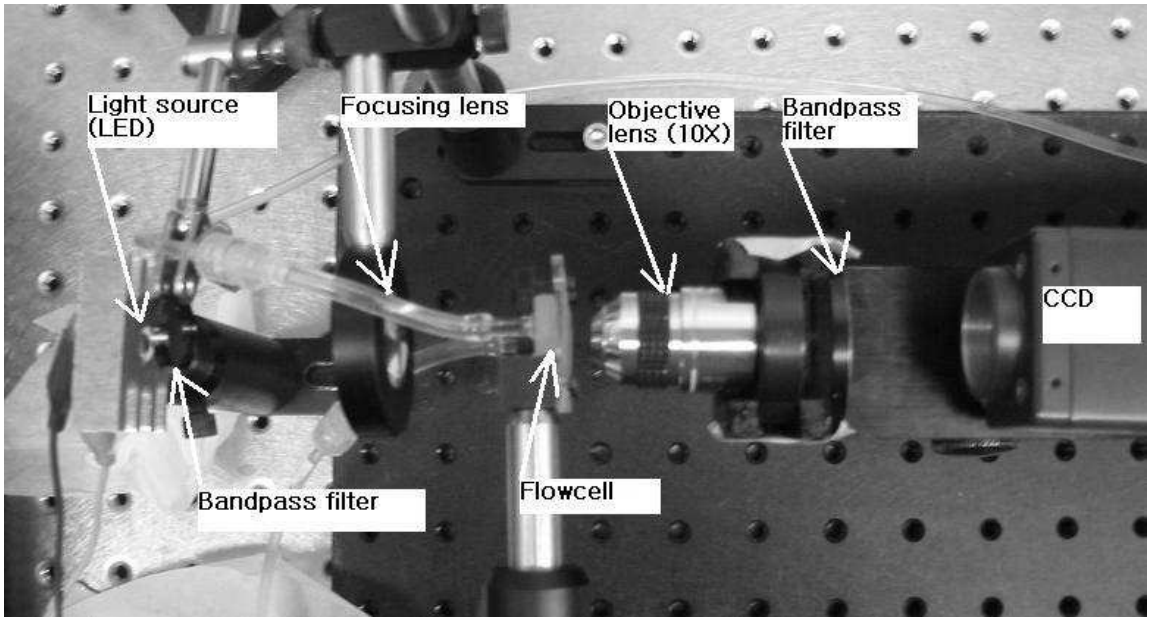

Figure 3.1. An optical setup for the fluorescence imaging system.

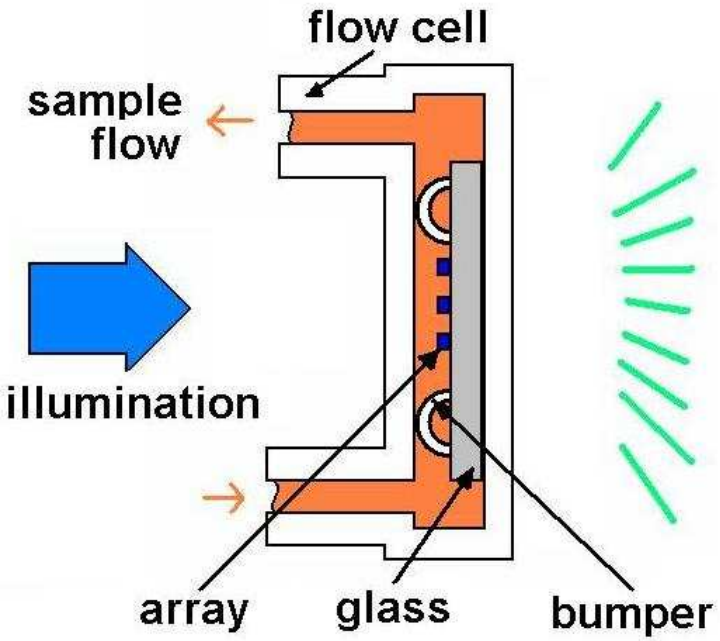

Figure 3.2. A diagram of the flow cell with a hydrogel microarray.

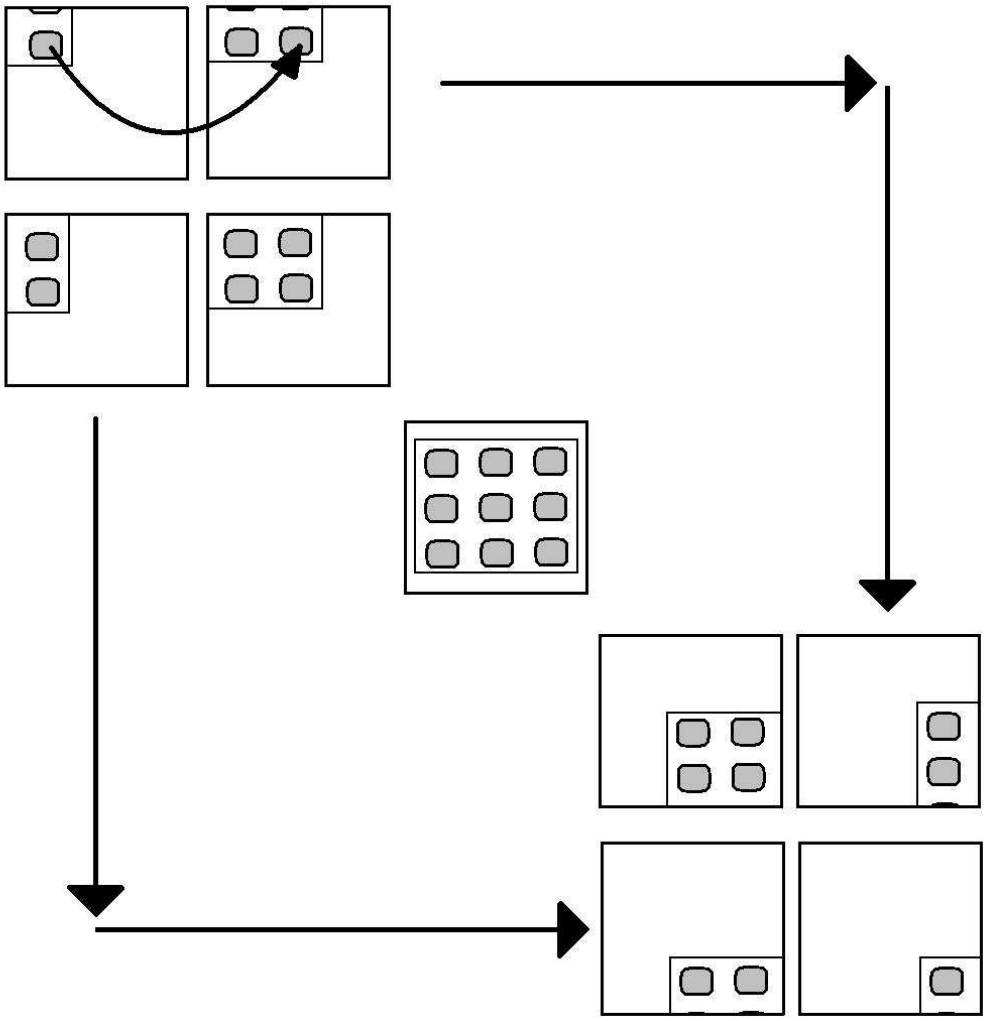

Figure 3.3. A diagram of the procedure for the spatial uniformity test.

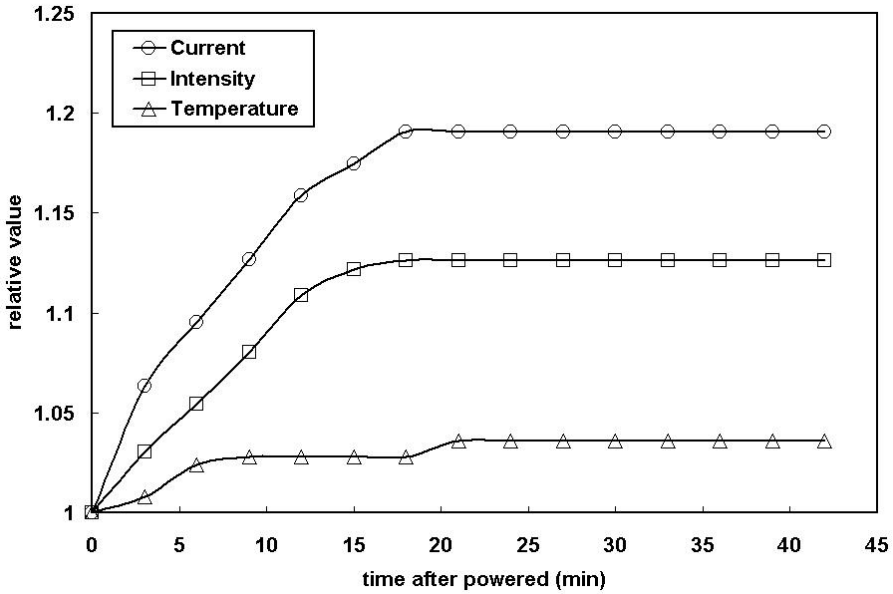

(a)

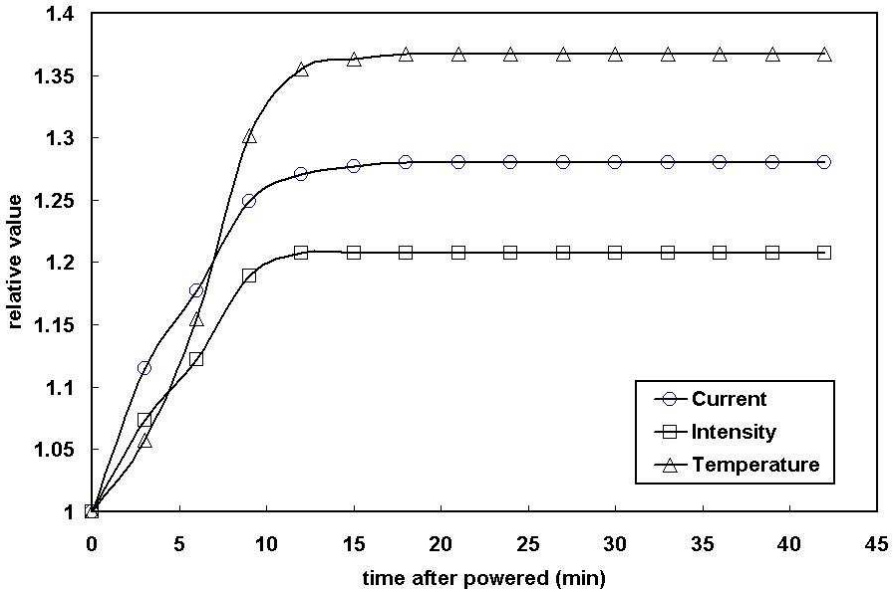

(b)

Figure 3.4. The results from the LED stability test at 3 V (a) and 3.5 V (b).

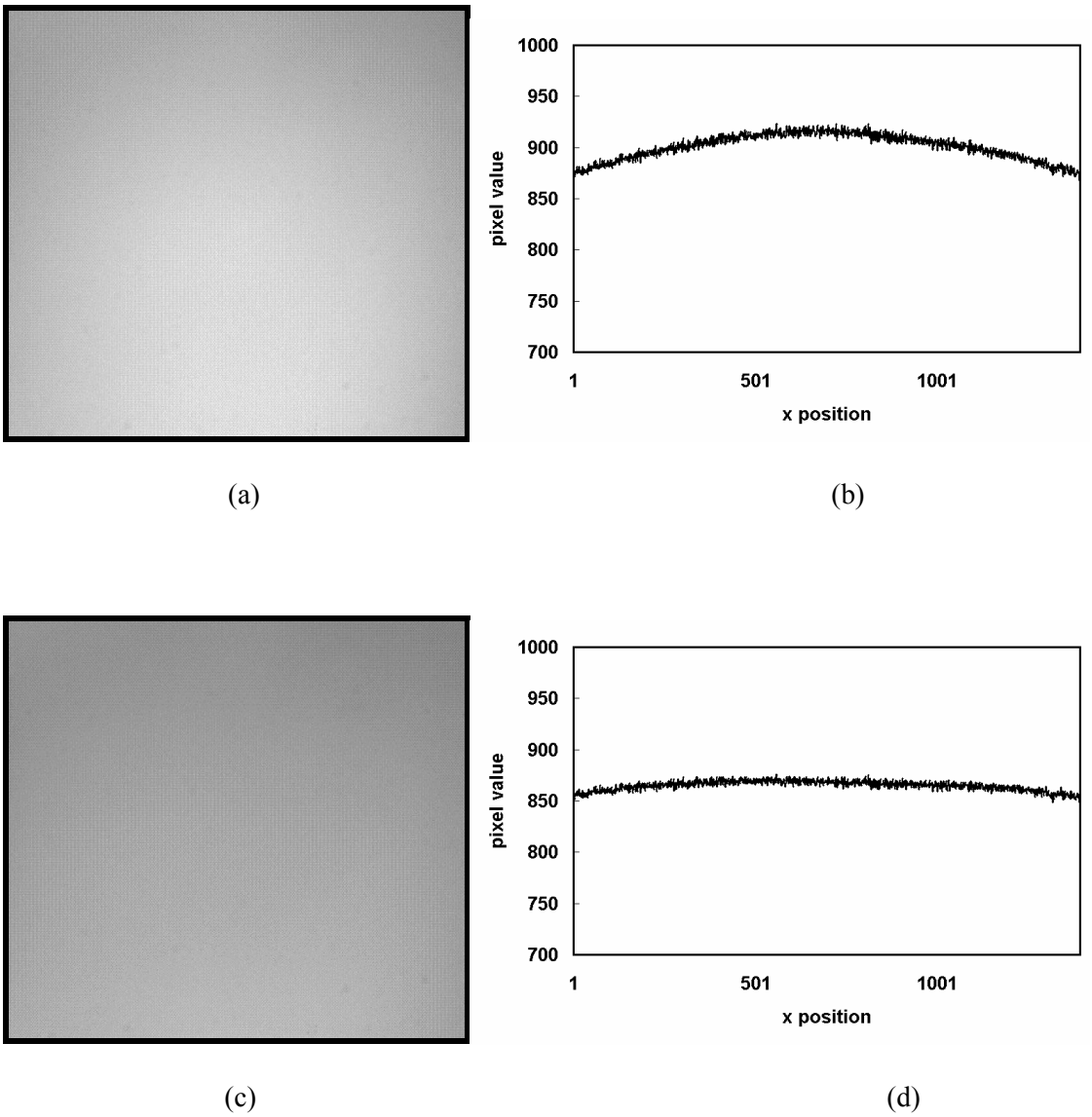

Figure 3.5. Intensity image of the LED (a), middle intensity profile (b), intensity image using a diffusion film (c), and middle intensity profile using a diffusion film (d).

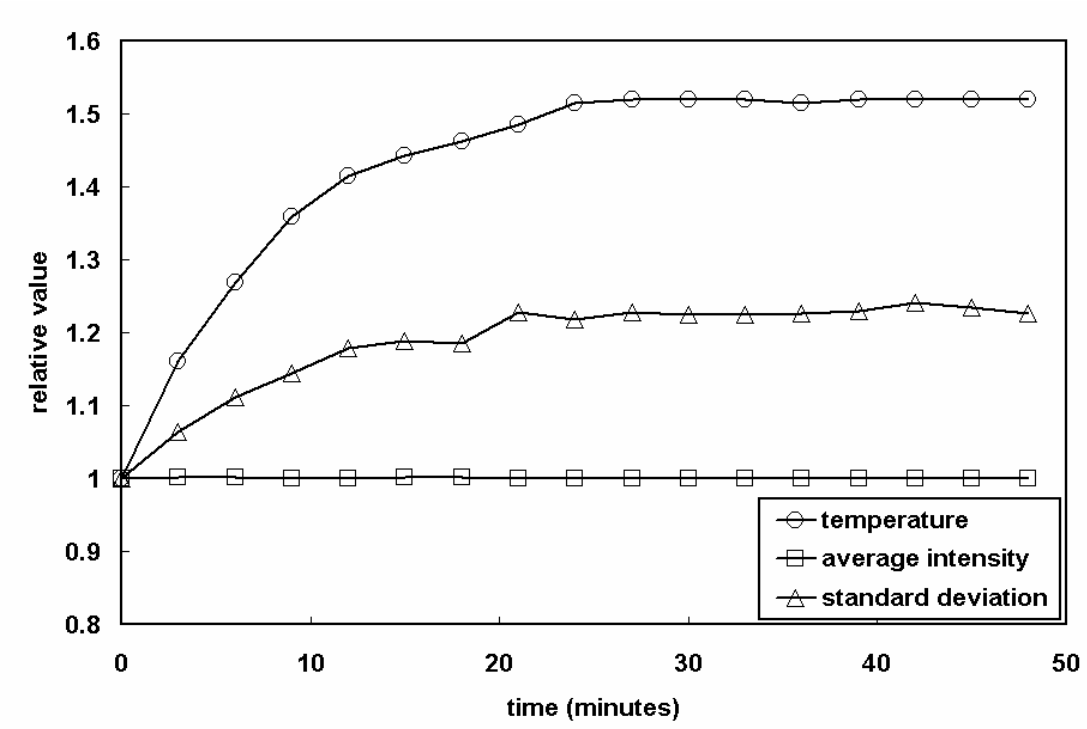

Figure 3.6. The results from camera stability test.

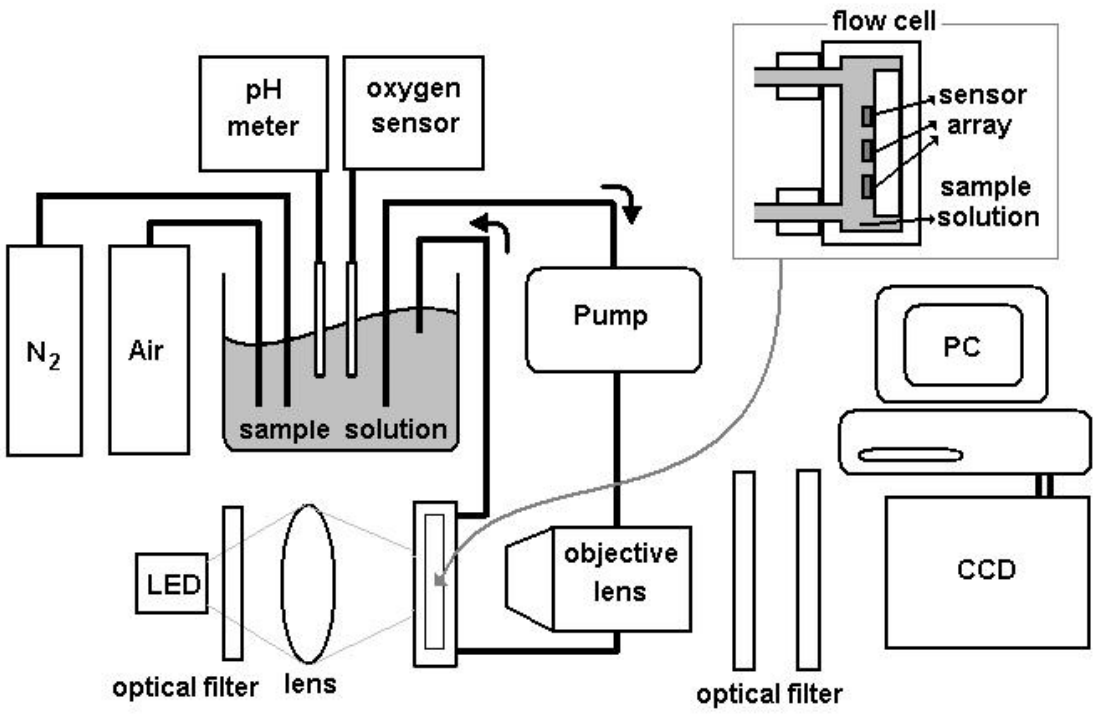

Figure 4.1. The experimental setup for characterization of a multi-analyte sensitive hydrogel microarray sensor.

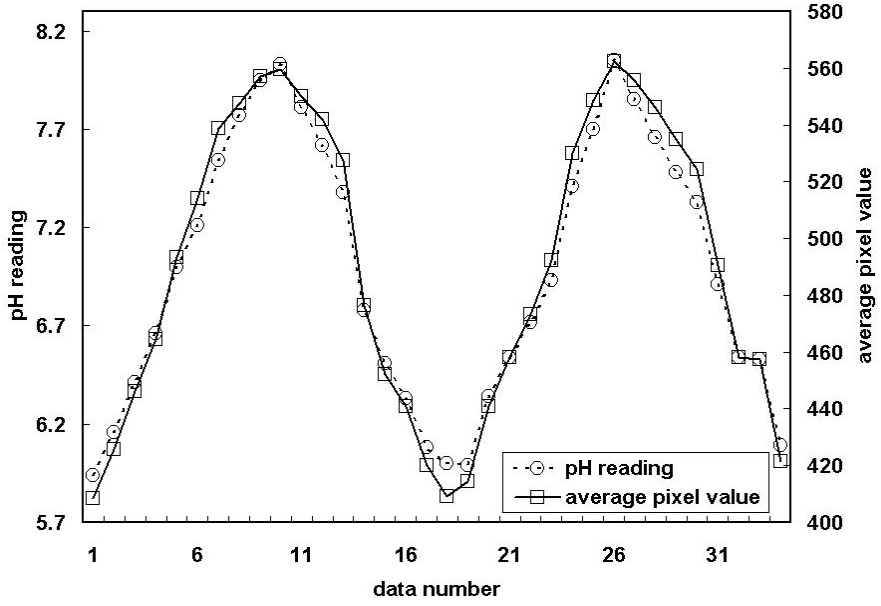

Figure 4.2. The response of the BCECF sensing element to a controlled pH titration in a PBS solution.

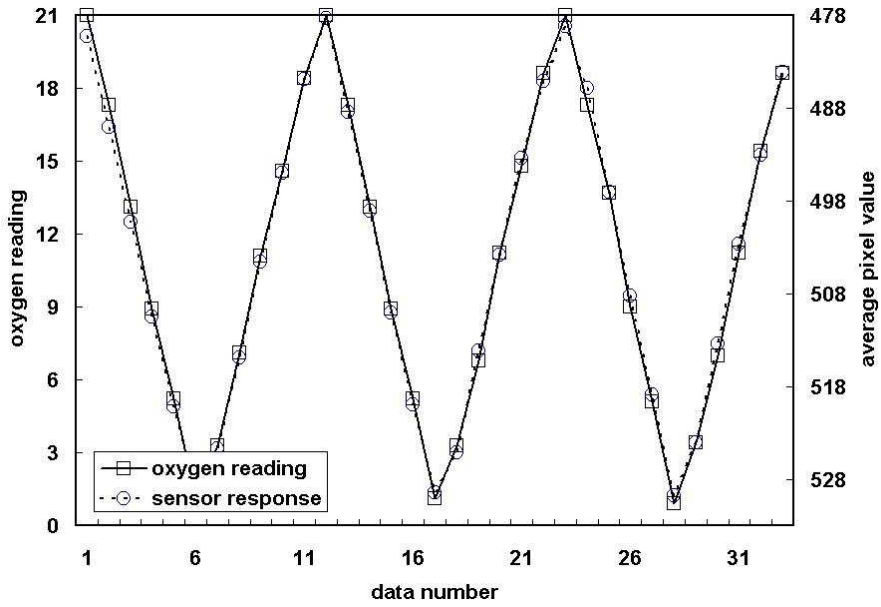

Figure 4.3. The response of the Ruthenium complex sensing element to a controlled O_2 titration in a PBS solution.

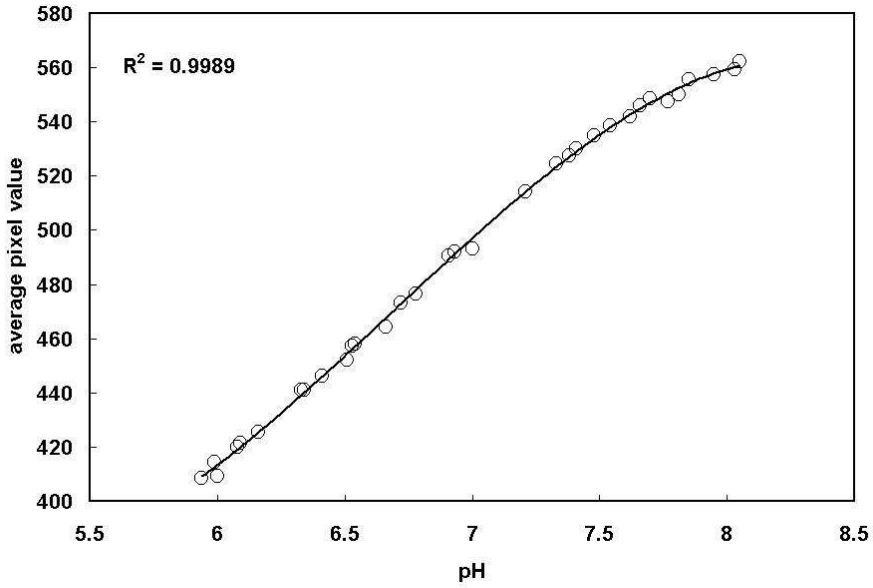

Figure 4.4. The calibration model of the pH sensor in a PBS solution.

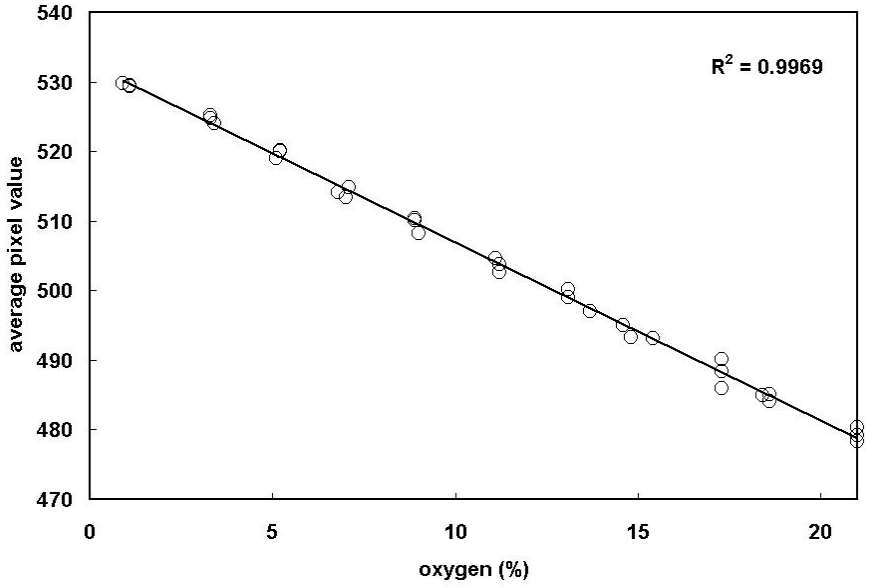

Figure 4.5. The calibration model of the O_2 sensor in a PBS solution.

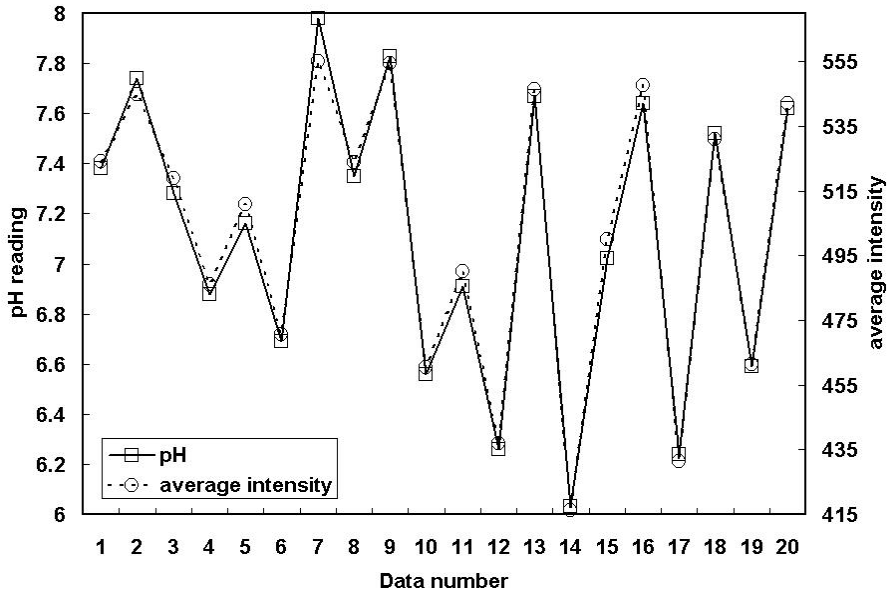

Figure 4.6. The response of the BCECF sensing element to a randomly spiked pH titration in a PBS solution.

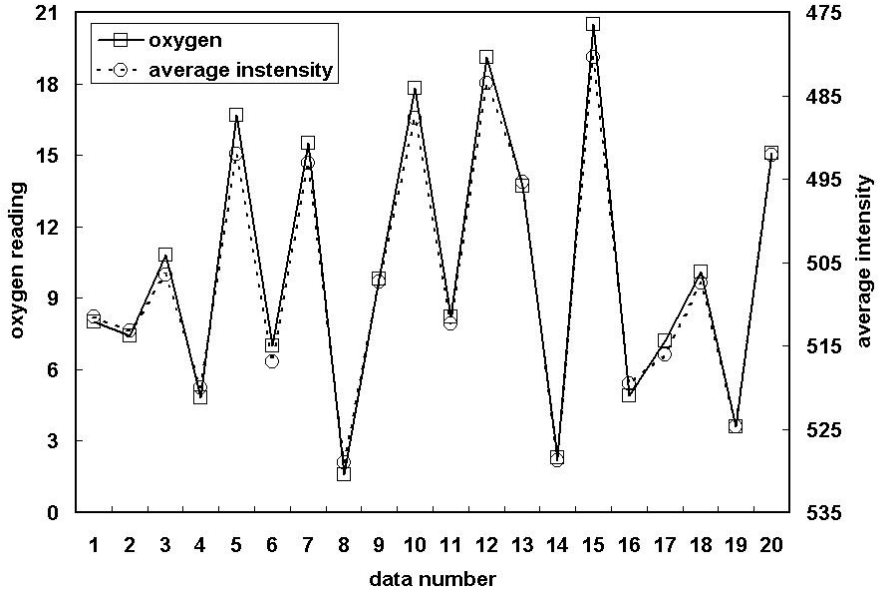

Figure 4.7. The response of the Ruthenium complex sensing element to a randomly spiked O_2 titration in a PBS solution.

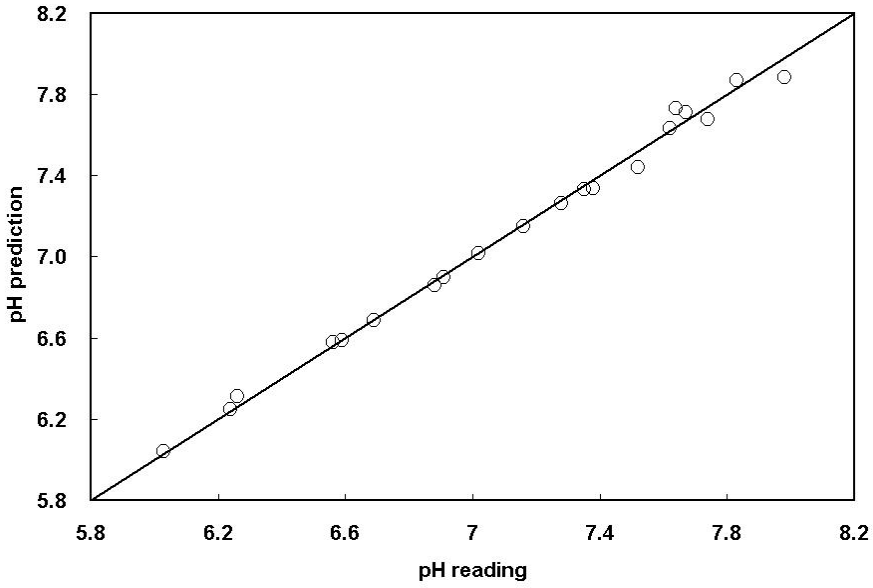

Figure 4.8. Prediction data of the pH sensor in a PBS solution.

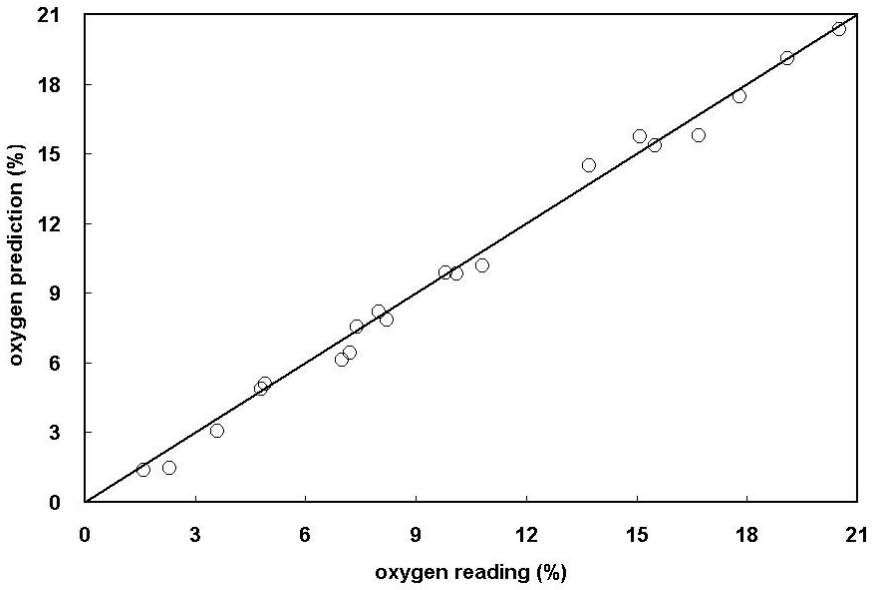

Figure 4.9. Prediction data of the O_2 sensor in a PBS solution.

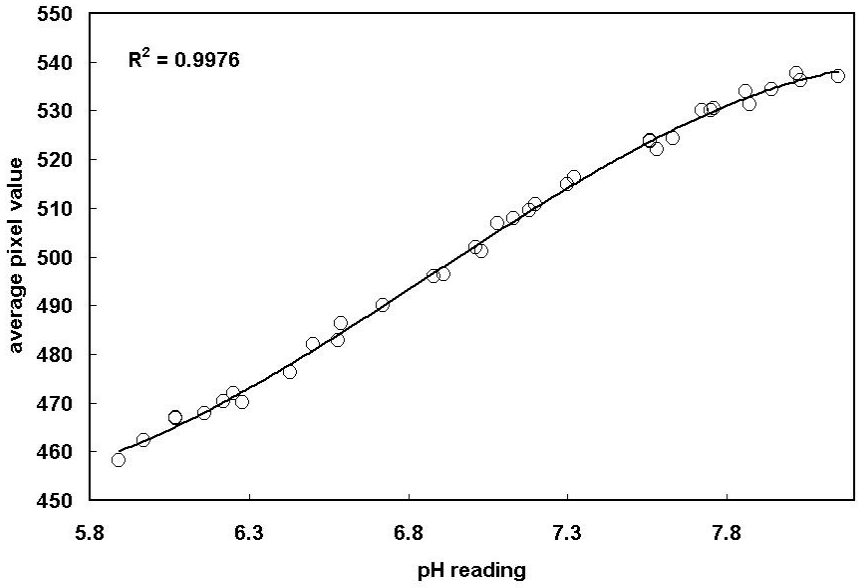

Figure 4.10. The calibration model of the pH sensor in MEM.

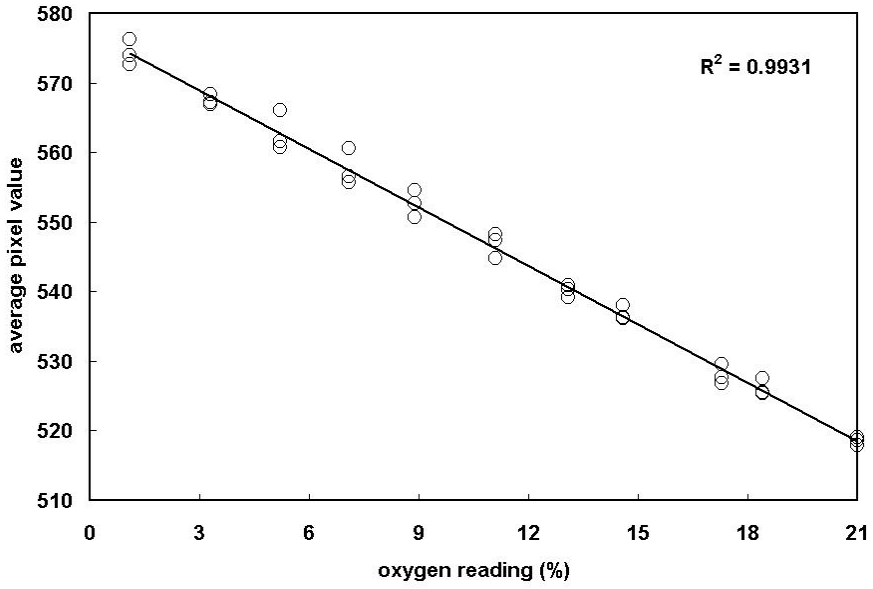

Figure 4.11. The calibration model of the O_2 sensor in MEM.

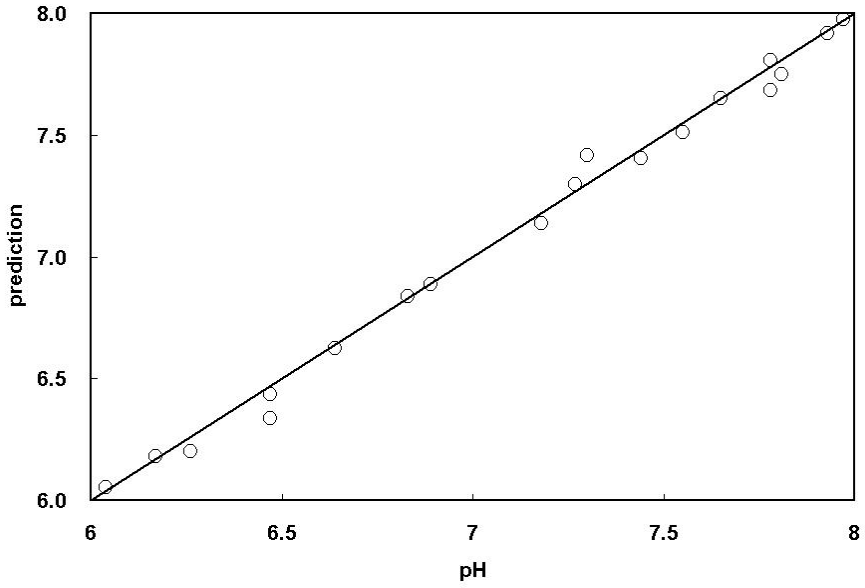

Figure 4.12. Prediction data of the pH sensor in MEM.

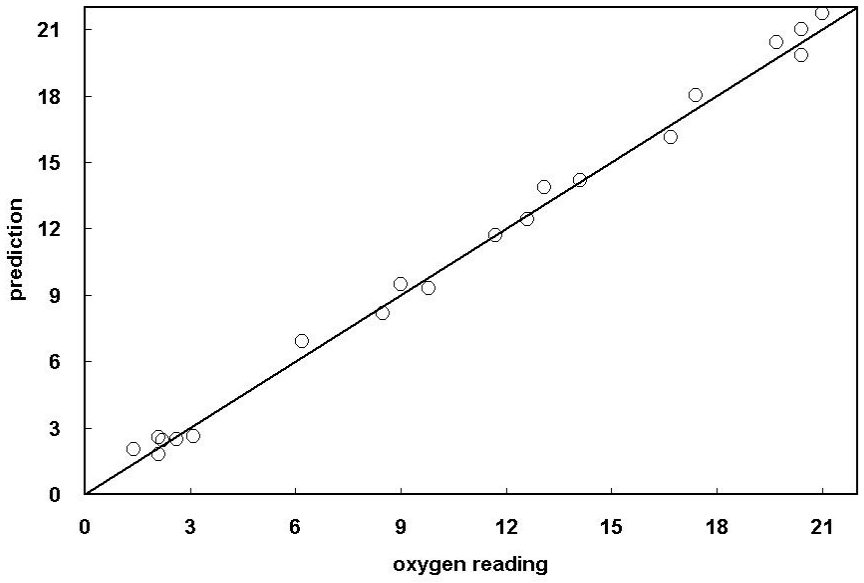

Figure 4.13. Prediction data of the O_2 sensor in MEM.

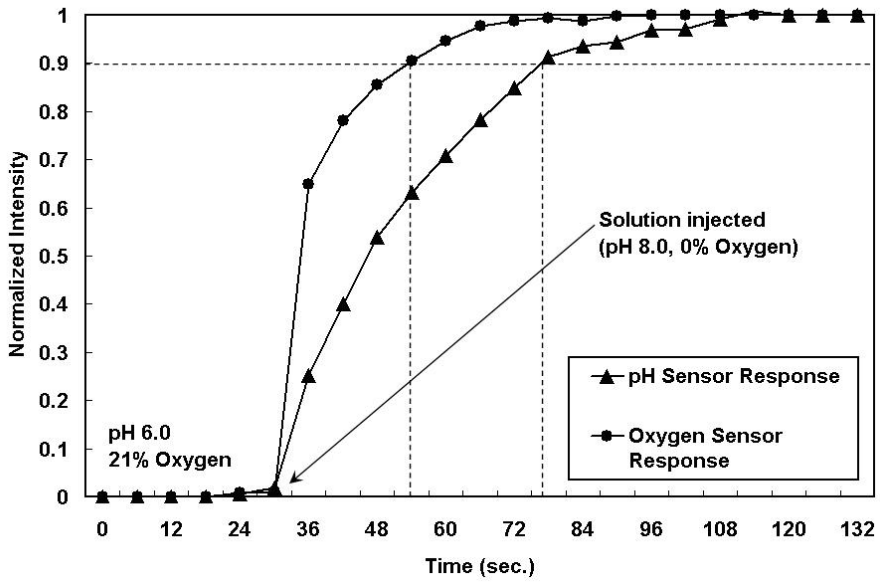

Figure 4.14. The time response of the sensor from the minimum to maximum intensity within the range of interest (0-21% oxygen and 6-8 pH).

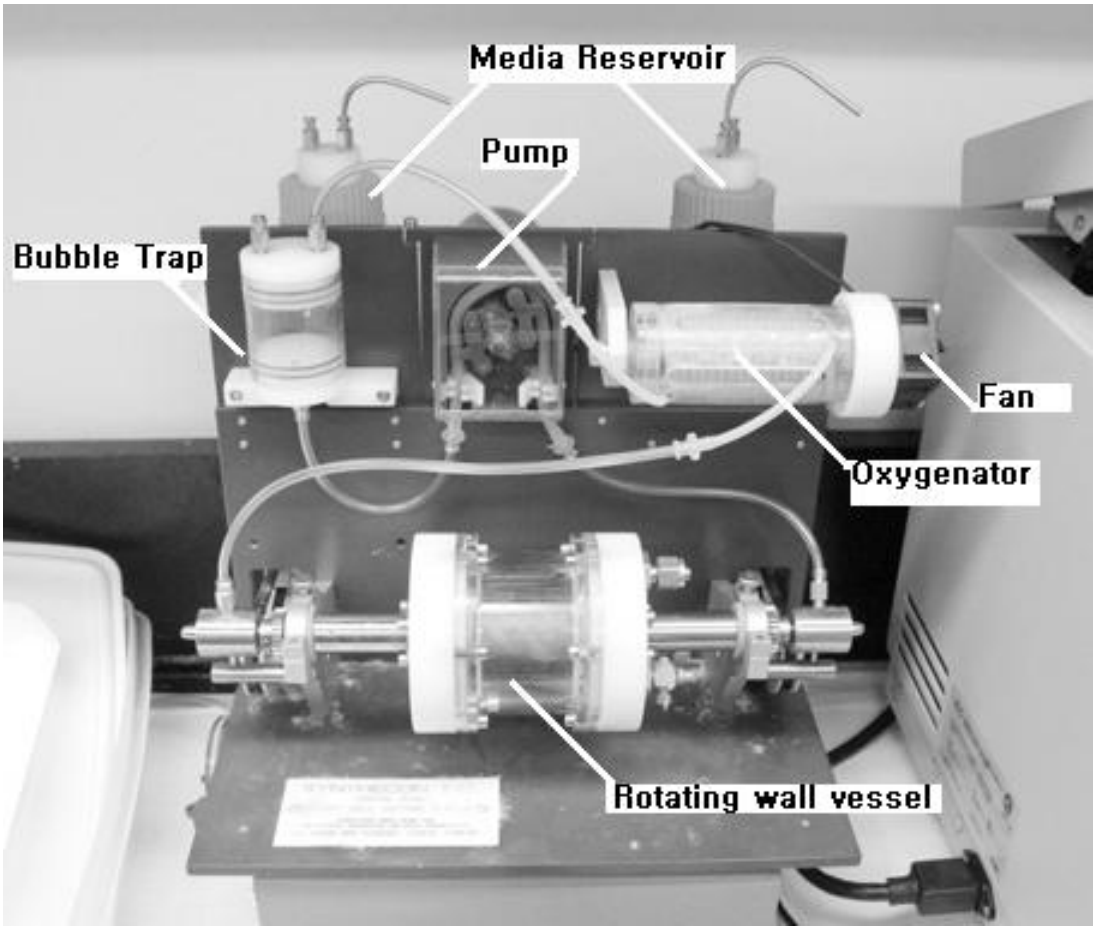

Figure 5.1. Synthecon rotary cell culture system.

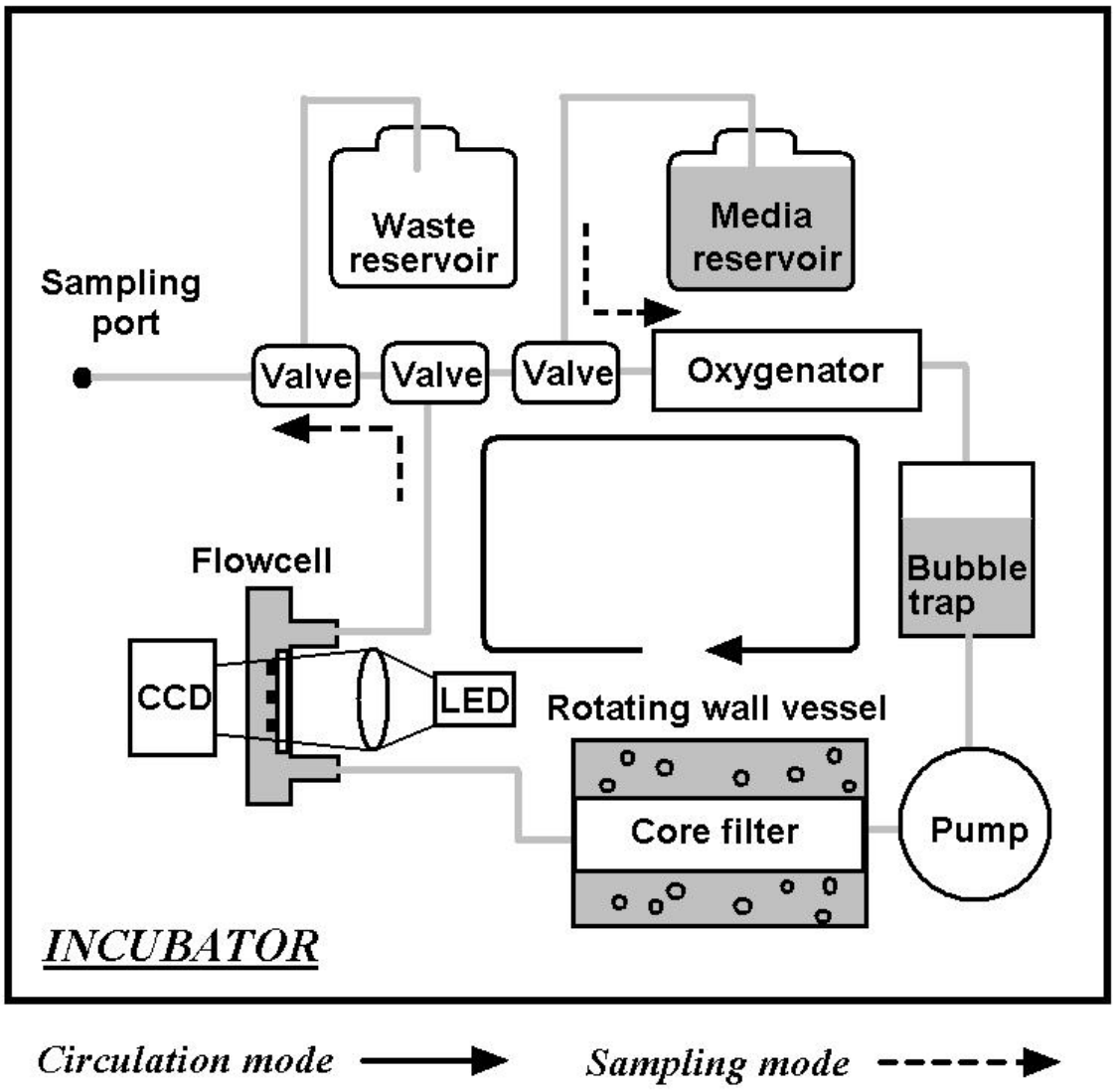

Figure 5.2. A diagram of optical setup coupled with a bioreactor.

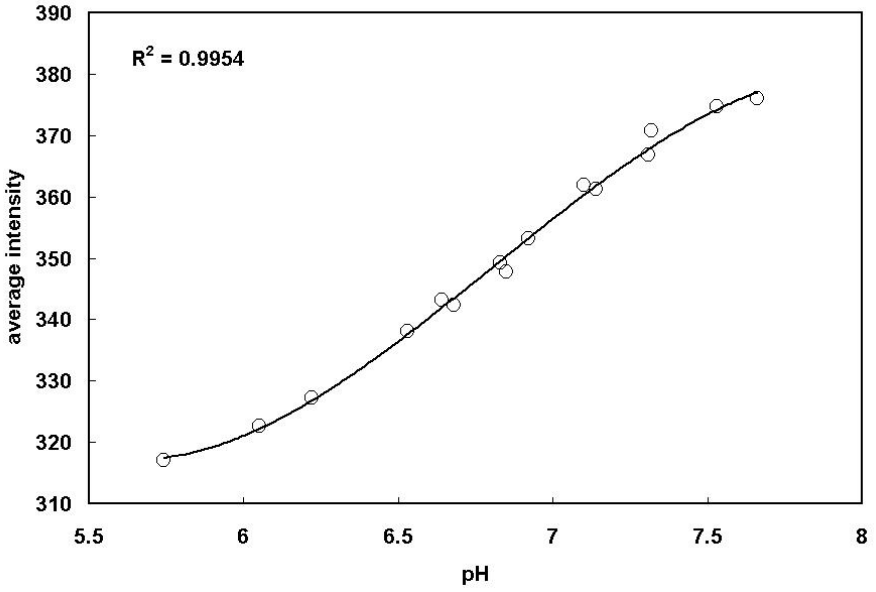

Figure 5.3. Calibration model for the pH sensor.

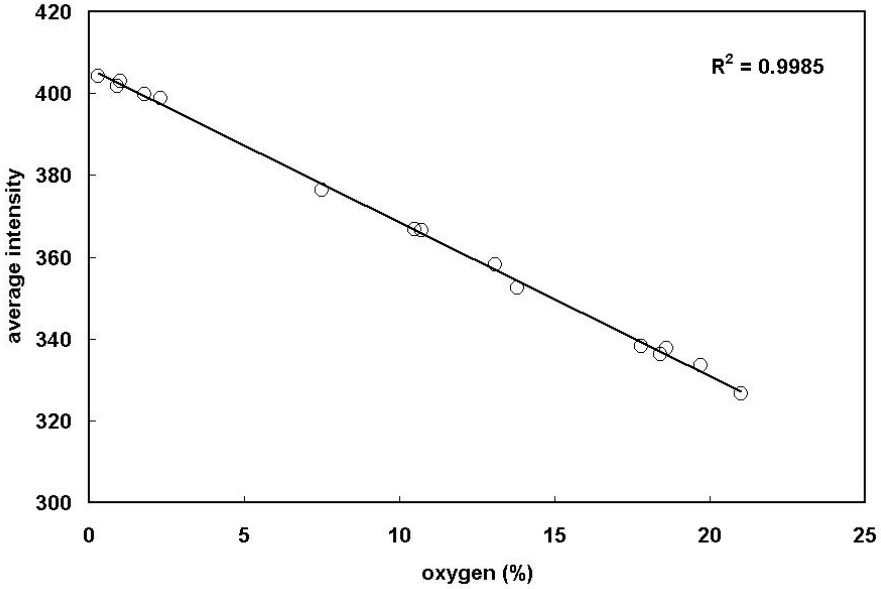

Figure 5.4. Calibration model for the O_2 sensor.

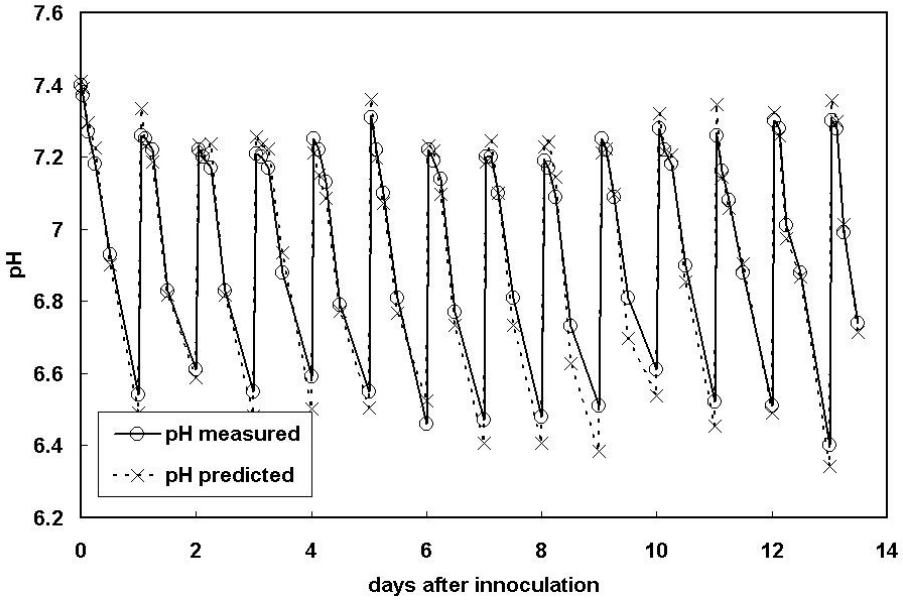

Figure 5.5. pH sensor response during a bioprocess.

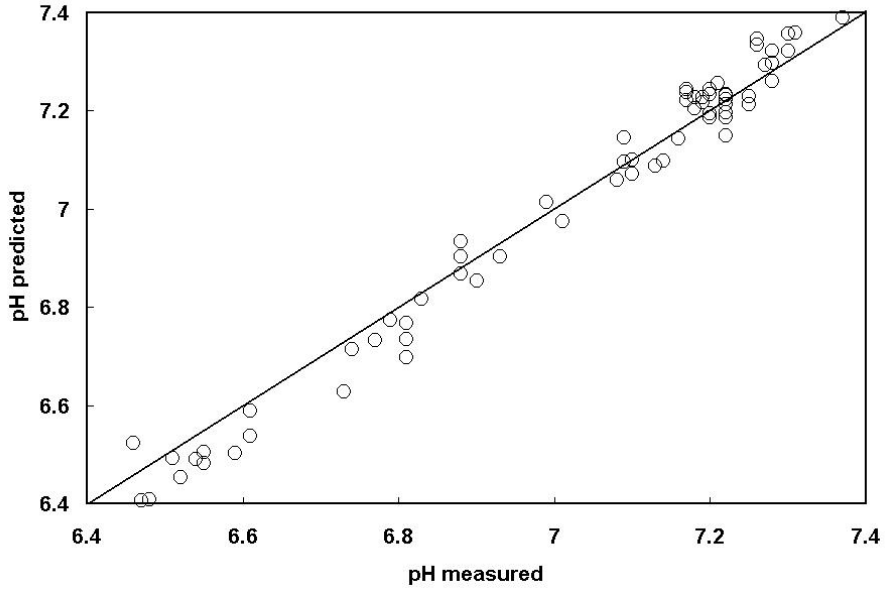

Figure 5.6. Prediction data from the pH sensor during a bioprocess.

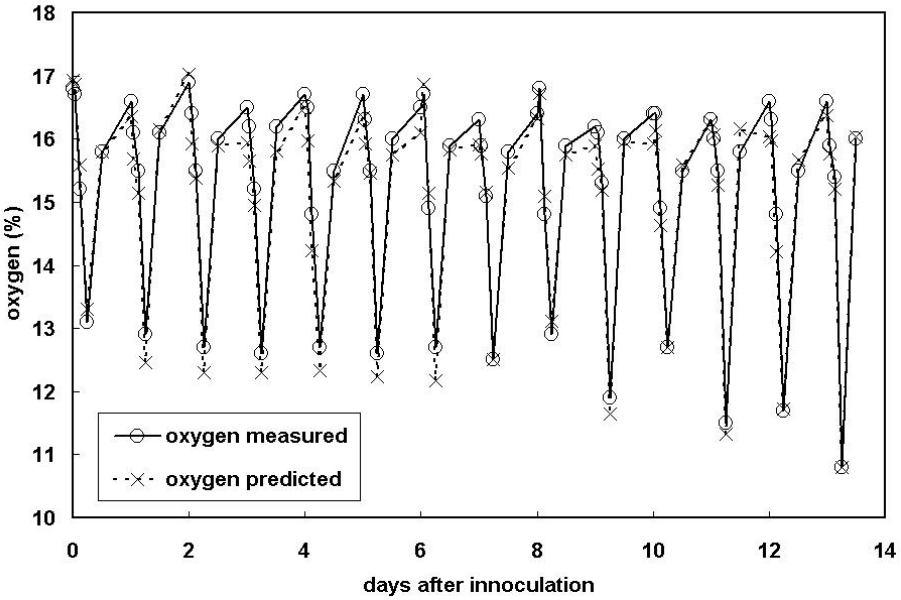

Figure 5.7. O_2 sensor response during a bioprocess.

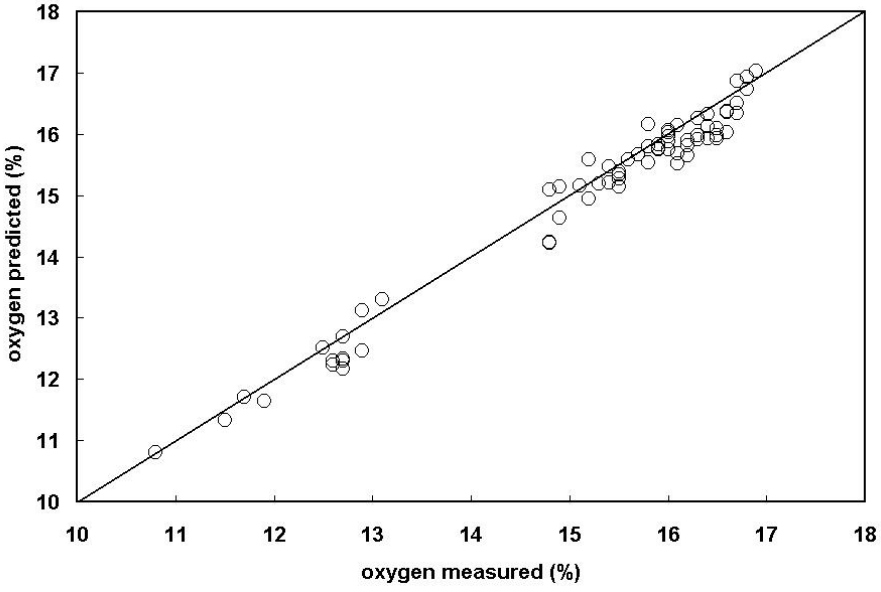

Figure 5.8. Prediction data from the O_2 sensor during a bioprocess.

APPENDIX B

Table 3.1. The results from spatial uniformity test of the sensor.

			HORIZONTAL POSITION		
			LEFT	MIDDLE	RIGHT
VERTICAL POSITION	TOP	1st element	403.701	410.831	401.217
		2nd element	403.453	410.241	401.807
		3rd element	404.486	411.066	401.356
		4th element	403.702	410.001	402.008
		5th element	403.972	410.005	401.849
		6th element	402.719	410.504	401.106
		7th element	404.594	411.331	401.986
		8th element	403.550	410.428	401.102
		9th element	403.812	410.727	401.209
		Standard deviation	**0.559**	**0.460**	**0.388**
	MIDDLE	1st element	409.537	420.242	411.220
		2nd element	410.022	419.514	411.307
		3rd element	410.054	421.033	411.211
		4th element	409.258	420.126	411.189
		5th element	409.240	420.025	411.679
		6th element	408.860	420.877	412.019
		7th element	408.692	420.652	411.780
		8th element	409.973	420.520	412.043
		9th element	409.486	419.730	411.916
		Standard deviation	**0.497**	**0.511**	**0.364**
	BOTTOM	1st element	402.721	412.222	404.771
		2nd element	402.976	411.670	405.128
		3rd element	401.947	411.370	404.778
		4th element	402.751	411.663	405.320
		5th element	402.931	412.508	405.369
		6th element	402.995	412.181	404.269
		7th element	401.858	412.080	405.376
		8th element	401.758	413.206	405.452
		9th element	403.107	412.212	405.437
		Standard deviation	**0.545**	**0.539**	**0.409**

Table 4.1 Standard error of calibration (SEC) and standard error of prediction (SEP) for pH and dissolved oxygen in buffer and cell culture media.

	Buffer (PBS)		Cell culture media (MEM)	
	pH	Oxygen (%)	pH	Oxygen (%)
SEC	0.0682	0.621	0.0712	0.624
SEP	0.0702	0.639	0.0713	0.648

Table 5.1. The actual pH and dissolved oxygen values for spiked calibration data.

Data number	O_2 (%)	pH
1	2.3	7.32
2	18.6	7.66
3	0.3	7.1
4	10.7	6.92
5	18.4	6.85
6	21	6.68
7	13.8	6.22
8	13.1	6.05
9	7.5	5.74
10	10.5	6.53
11	1	6.83
12	0.9	7.14
13	17.8	7.31
14	19.7	7.53
15	1.8	6.64
	Correlation (R^2) = 0.109	

Table 5.2. The results from the pH and O_2 sensors during a bioprocess.

	pH sensor	O_2 sensor (%)
SEC	0.061	0.554
SEP	0.092	0.721

VITA

Seung Joon Lee was born and raised in Seoul, Korea. He received a B.S. degree in Mechanical Engineering from Yonsei University, Seoul, Korea in February 2000. After he received his B.S., he attended Texas A&M University in College Station and received a M.S. degree in Biomedical Engineering in May 2003. After receiving his M.S. degree, he continued his Ph.D. degree at the same University and received his Ph.D. in Biomedical Engineering in December 2006.

Permanent Address: 312-1103 Hyundai Apartment,
Chungsong-Maeul, Jangki-Dong, Kimpo-Si
Kyungki-Do, Republic of Korea

E-mail: sjlee94@yahoo.com